Vision Research 50 (2010) 698–715

Contents lists available at ScienceDirect

Vision Research

journal homepage: www.elsevier.com/locate/visres

Convergence of linkage, gene expression and association data demonstrates the influence of the RAR-related orphan receptor alpha (*RORA*) gene on neovascular AMD: A systems biology based approach

Alexandra C. Silveira [a], Margaux A. Morrison [a], Fei Ji [b], Haiyan Xu [b], James B. Reinecke [c], Scott M. Adams [a], Trevor M. Arneberg [a], Maria Janssian [a], Joo-Eun Lee [a], Yang Yuan [c], Debra A. Schaumberg [d], Maria G. Kotoula [e], Evangeline E. Tsironi [e], Aristoteles N. Tsiloulis [e], Dimitrios Z. Chatzoulis [e], Joan W. Miller [f], Ivana K. Kim [f], Gregory S. Hageman [g], Lindsay A. Farrer [h], Neena B. Haider [c], Margaret M. DeAngelis [a,*]

[a] *Ocular Molecular Genetics Institute and Department of Ophthalmology, Harvard Medical School, Massachusetts Eye and Ear Infirmary, Boston, MA, United States*
[b] *The Laboratory of Statistical Genetics, Rockefeller University, New York, NY, United States*
[c] *Department of Genetics, Cell Biology, and Anatomy, University of Nebraska Medical Center, Omaha, NE, United States*
[d] *Division of Preventive Medicine, Brigham and Women's Hospital, Boston, MA, United States*
[e] *Department of Ophthalmology, University of Thessaly School of Medicine, Larissa, Greece*
[f] *Retina Service and Department of Ophthalmology, Harvard Medical School, Massachusetts Eye and Ear Infirmary, Boston, MA, United States*
[g] *Department of Ophthalmology and Visual Sciences, Cell Biology and Functional Genomics Laboratory, The University of Iowa, Iowa City, IA, United States*
[h] *Departments of Medicine (Genetics), Neurology, Genetics and Genomics, Epidemiology, and Biostatistics, Boston University Schools of Medicine and Public Health, Boston, MA, United States*

ARTICLE INFO

Article history:
Received 17 June 2009
Received in revised form 4 September 2009

Keywords:
Neovascularization
RORA
Single nucleotide polymorphisms
Haplotypes
Linkage
Microarray

ABSTRACT

To identify novel genes and pathways associated with AMD, we performed microarray gene expression and linkage analysis which implicated the candidate gene, retinoic acid receptor-related orphan receptor alpha (*RORA*, 15q). Subsequent genotyping of 159 *RORA* single nucleotide polymorphisms (SNPs) in a family-based cohort, followed by replication in an unrelated case-control cohort, demonstrated that SNPs and haplotypes located in intron 1 were significantly associated with neovascular AMD risk in both cohorts. This is the first report demonstrating a possible role for *RORA*, a receptor for cholesterol, in the pathophysiology of AMD. Moreover, we found a significant interaction between *RORA* and the *ARMS2/HTRA1* locus suggesting a novel pathway underlying AMD pathophysiology.

1. Introduction

The etiology of age-related macular degeneration (AMD) has yet to be fully elucidated; nevertheless, it is clear that the development and progression of this complex, multifactorial disease may be influenced by several different pathways, including cholesterol and lipid metabolism (for reviews please see Ding, Patel, & Chan, 2009; Javitt & Javitt, 2009). Epidemiologic findings have indicated a role for lipid/cholesterol metabolism in the pathogenesis of AMD (Baker et al., 2009; Klein, Klein, & Jensen, 1997; Tan, Wang, Flood, & Mitchell, 2009). This is further supported by evidence that comes from studies showing that the use of cholesterol lowering drugs (statins) has a protective effect against the development of neovascular AMD and all types of AMD (McGwin, Xie, & Owsley, 2005; Wilson, Schwartz, Bhatt, McCulloch, & Duncan, 2004); however, others have found no significant association between use of these drugs and any AMD subtypes (Klein, Klein, Tomany, Danforth, & Cruickshanks, 2003; van Leeuwen, Vingerling, Hofman, de Jong, & Stricker, 2003). Additionally, both *in vivo* and *in vitro* assays have implicated a role for cholesterol/lipid metabolism in the development of AMD (Mullins, Russell, Anderson, & Hageman, 2000; Sallo et al., 2009; Yamada et al., 2008; Yu, Lorenz, Haritoglou, Kampik, & Welge-Lussen, 2009; for review please see Ding et al., 2009).

Genetic studies have similarly implicated several lipid/cholesterol metabolism and transport genes in the pathophysiology of early and/or advanced stages of AMD. For example, the genes toll-like receptors -3 and -4 (Yang et al., 2008; Zareparsi et al., 2005), apolipoprotein E (Anderson et al., 2001; Baird, Guida, Chu, Vu, & Guymer, 2004; Klaver et al., 1998; Schmidt et al., 2002;

* Corresponding author. Address: Department of Ophthalmology, Harvard Medical School, Massachusetts Eye and Ear, 243 Charles Street, Boston, MA 02114, United States. Fax: +1 617 573 4352.
E-mail address: margaret_deangelis@hms.harvard.edu (M.M. DeAngelis).

0042-6989/$ - see front matter © 2009 Elsevier Ltd. All rights reserved.
doi:10.1016/j.visres.2009.09.016

Souied et al., 1998; Zareparsi et al., 2004), ATP-binding cassette transporter (Allikmets, 2000; Allikmets et al., 1997) and the elongation of very long chain fatty acids-like 4 (Conley et al., 2005) have all been associated with risk of all AMD subtypes. However, these findings have not been replicated consistently (Allikmets et al., 2009; Ayyagari et al., 2001; Cho, Chew, Mitchell, & Tuo, 2009; De La Paz et al., 1999; DeAngelis et al., 2007; Despriet et al., 2008; Edwards, Swaroop, & Seddon, 2009; Edwards et al., 2008; Guymer et al., 2001; Haddad, Chen, Santangelo, & Seddon, 2006; Lewin, 2009; Liew, Mitchell, & Wong, 2009; Schultz et al., 2003; Souied et al., 2000; Stone et al., 1998).

The variants and haplotypes most consistently associated with AMD are within the gene complement factor H (*CFH*) (1q32) and the locus containing the genes age-related maculopathy susceptibility 2 and HtrA serine peptidase 1 (*ARMS2* and *HTRA1*) (10q26) (DeAngelis et al., 2008; Dewan et al., 2006; Edwards et al., 2005; Hageman et al., 2005; Haines et al., 2005; Jakobsdottir et al., 2005; Kanda et al., 2007; Klein et al., 2005; Li et al., 2006; Rivera et al., 2005; Yang et al., 2006). These genes have been shown to have large influences on AMD risk in populations of various ethnicities, with variants on 10q26 being the most strongly associated with the neovascular AMD subtype (Fisher et al., 2005; Shuler et al., 2007; Zhang et al., 2008). Despite their large influence on AMD risk, the combination of these genes alone is insufficient to correctly predict the development and progression of this disease (Jakobsdottir, Gorin, Conley, Ferrell, & Weeks, 2009). While additional genes may be only minor players in terms of their contribution to the total genetic variance of AMD, effect size does not always correlate with the importance to pathogenesis of AMD. Additionally, because other loci do exist which have yet to be elucidated (Abecasis et al., 2004; Fisher et al., 2005; Iyengar et al., 2004; Jun et al., 2005; Kenealy et al., 2004; Majewski et al., 2003; Schick et al., 2003; Schmidt et al., 2004; Seddon, Santangelo, Book, Chong, & Cote, 2003), it is clear that the percent of genetic variance is not proportional to understanding the pathophysiology of disease or understanding gene–gene interactions. It may therefore be important to identify and characterize additional risk factors that may augment the value of known risk factors as prognostic tools in order to identify individuals that require closer follow-up and early intervention (Jakobsdottir et al., 2009; Ware, 2006). Moreover, it is equally important to determine the mechanism of disease, not just risk factors, so that appropriate avenues for treatment may be identified and explored.

Retinoic acid receptor-related orphan receptor alpha (*RORA*) is one of three retinoid-related orphan receptors that compose a distinct subfamily of nuclear receptors (Hubbard et al., 2009). *RORA* is known to play a key role in the regulation of circadian rhythms, the development of cones, bone morphogenesis, angiogenesis, and pathways including immunity/inflammation, lipid metabolism, and cholesterol (Besnard et al., 2001, 2002; Boukhtouche, Mariani, & Tedgui, 2004; Boukhtouche et al., 2006; Lau et al., 2008; Zhu, McAvoy, Kuhn, & Smith, 2006).

In vitro studies have identified cholesterol as a natural ligand of *RORA* (Kallen et al., 2002). In addition to binding cholesterol, *RORA* has also been shown to regulate lipoproteins, such as high density lipoprotein, serum amyloid A, and apolipoprotein A1 (Lau et al., 2008; Migita, Satozawa, Lin, Morser, & Kawai, 2004; Voyiaziakis et al., 1998). Further evidence for the role of *RORA* in cholesterol (“cholesteROR”) metabolism comes from phenotypic examination of the *RORA* deficient *staggerer* mouse (*RORA*^{sg}) that displays an increased susceptibility to arteriosclerosis and dislipidemia (Boukhtouche et al., 2004; Jetten & Ueda, 2002; Kopmels, Mariani, Taupin, Delhaye-Bouchaud, & Wollman, 1991; Lau et al., 2008; Mamontova et al., 1998).

If cholesterol/lipid transport and metabolism are involved in the pathophysiology of neovascular AMD, then genes that are intrinsic to these pathways may be differentially expressed between patients with neovascular AMD and their unaffected siblings. In order to identify novel candidate genes and pathways with biological relevance to AMD pathophysiology, we performed linkage analysis and gene expression microarray analysis on extremely discordant sibling pairs. An “extreme” sibling pair consists of one sibling with a trait value in the top 10% of disease severity and the other sibling with a trait value in the bottom 10% of disease severity (Risch & Zhang, 1995, 1996). Based on the results of these studies and biological plausibility in AMD etiology, the candidate gene *RORA* was chosen for further analysis. Any significant haplotypes identified in the family-based cohort of European descent were then tested in an unrelated case-control cohort from Central Greece.

2. Methods

2.1. Family patient population

The protocol was reviewed and approved by the Institutional Review Boards at Massachusetts Eye and Ear Infirmary, Boston, Massachusetts and conforms to the tenets of the Declaration of Helsinki. Eligible patients were enrolled in this study after they gave informed consent, either in person, over the phone, or through the mail, before completing a standardized questionnaire and donating 10–50 ml of venous blood.

Details for the recruitment of the 196 sibling pairs, comprised mainly of individuals of European ancestry, are described elsewhere (DeAngelis et al., 2008) (Population characteristics are summarized in Supplementary Table 1). In brief, all index patients were aged 50 years or older, except where one individual was 49 years of age, and had the neovascular form of AMD in at least one eye, defined by subretinal hemorrhage, fibrosis, or fluorescein angiographic presence of neovascularization documented at the time of, or prior to, enrollment in the study. Patients whose only exudative finding was a retinal pigment epithelium detachment were excluded because this finding may not represent definite neovascular AMD. Patients with signs of pathologic myopia, presumed ocular histoplasmosis syndrome, angioid streaks, choroidal rupture, any hereditary retinal diseases other than AMD, and previous laser treatment due to retinal conditions other than AMD were also excluded.

Of the 196 sibling pairs, 150 were extremely phenotypically discordant. That is pairs where the unaffected siblings had normal maculae at an age older than that at which the index patient was first diagnosed with neovascular AMD. Normal maculae (defined as the zone centered at the foveola and extending two disk diameters, or 3000 μm, in radius) fulfilled the following criteria: 0–5 small drusen (all less than 63 μm in diameter), no pigment abnormalities, no geographic atrophy, and no neovascularization [as defined previously; AMD “category 1 or less” on the Age-Related Eye Disease Study (AREDS) scale (AREDS Research Group, 2000)]. Disease status of every participant was confirmed by at least two of the investigators by evaluation of fundus photographs or fluorescein angiograms except when one of the investigators directly examined an unaffected sibling during a home visit ($n = 4$ cases). Smoking data, as measured in pack years, was available for every participant.

An additional 46 discordant sibling pairs were analyzed where each pair was comprised of one sibling (the index sibling) with neovascular AMD and the other sibling (the control sibling) with mild or very early AMD [AREDS category 2 (AREDS Research Group, 2000)] at 65 years of age or older in most cases. Siblings were categorized as early AMD only if they met the following criteria for the definition of AREDS category 2: small (<63 μm) drusen with total area $\geqslant$125 μm diameter circle, or at least one intermediate

drusen (⩾63 and <125 μm) or presence of pigment. These criteria are based on published epidemiologic studies that indicate that elderly individuals with such maculae rarely go onto develop neovascular AMD during a 10 year follow-up (Klein, Klein, Tomany, & Moss, 2002).

2.2. Unrelated case and control population

Replication of significant findings was performed on an unrelated case-control cohort from Central Greece that included patients without AMD, with early and intermediate dry AMD [AREDS category 2 (as described above) and AREDS category 3 (n = 84); intermediate drusen comprising total area ⩾360 μm diameter circle in the presence of soft drusen or ⩾656 μm diameter circle in absence of soft drusen, or at least one large druse (⩾125 μm), or non-Central geographic atrophy (AREDS Research Group, 2000)] and with neovascular AMD (cases, n = 139) (Supplementary Table 1). These patients were recruited from the medical retina outpatient clinic at the University Hospital of Larissa, Greece. The diagnosis of macular degeneration was confirmed by optical coherence tomography and fluorescein angiography. Color fundus photographs and indocyanine green angiography were performed in some cases.

2.3. Microarray analysis

Total RNA isolates from transformed lymphocyte cell lines derived from 18 individuals (nine sibpairs) were prepared using RNA-easy kits (Qiagen, Valencia, CA). Each pair was matched for smoking history, age, sex, cardiovascular disease history, body mass index, hypertension, and hypercholesterolemia, factors that could influence gene expression levels. RNA quality was determined by analysis using agarose gel or an Agilent 2100 Bioanalyzer instrument (Agilent, Santa Clara, CA). Approximately 20 μg of RNA was submitted to amplification, labeled, and hybridized to human Affymetrix U133A 2.0 PLUS microarrays (Affymetrix, Santa Clara, CA) containing analytical elements corresponding to approximately 35,000+ genes.

For the gene expression microarray analysis, statistical analysis was performed using principal component analysis (PCA) to identify substantial differences between the affected and unaffected siblings. Further analysis was performed employing a statistical tool referred to as robust multichip analysis (RMA). This procedure entailed the following: (1) probe-specific correction of the probes using a model based on observed intensity being the sum of signal and (background) noise (Irizarry et al., 2003), (2) normalization of corrected perfect match probes using quantile normalization

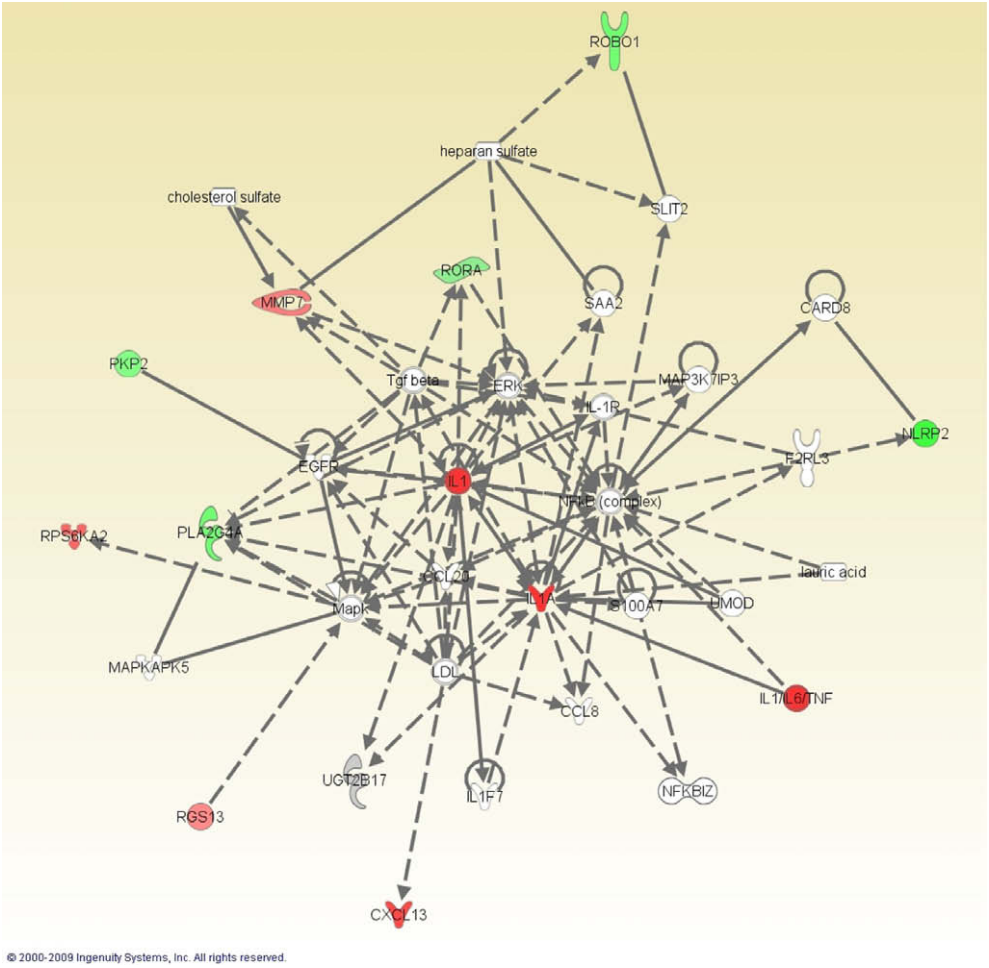

Fig. 1. IPA-generated network containing microarray genes that were identified as significant and that showed a greater than 2-fold difference when comparing neovascular AMD patients and their unaffected siblings. The molecules which are colored are those that were identified in our study. Green indicates down-regulation while red indicates up-regulation when comparing affected to unaffected siblings. Solid lines indicate direct relationships and dotted lines indicate indirect relationships as identified in previously published literature (http://www.ingenuity.com/index.html). The individual shapes represent the family of molecule, for example, the shape of *RORA* indicates a ligand-dependent nuclear receptor. A full listing of these proteins, their official name, and the family of molecules to which they belong can be found in Supplementary Table 3. (For interpretation of the references to colour in this figure legend, the reader is referred to the web version of this article.)

Table 1
Convergence of gene expression and genomic data.

Symbol	Entrez gene name	Statistical method	Direction of fold change[a]	Location	Genomic convergence evidence
CXCL13	Chemokine (C-X-C motif) ligand 13	GCRMA/LPE	Up	4q21	Linkage
IL1A	Interleukin 1, alpha	GCRMA/LPE	Up	2q14	
MMP7	Matrix metallopeptidase 7 (matrilysin, uterine)	GCRMA/LPE	Up	11q21-q22	
PKP2	Plakophilin 2	GCRMA	Down	12p11	
PLA2G4A	Phospholipase A2, group IVA (cytosolic, calcium-dependent)	GCRMA/LPE	Down	1q25	Linkage
NLRP2	NLR family, pyrin domain containing 2	GCRMA/LPE	Down	19q13.42	Linkage
RGS13	Regulator of G-protein signaling 13	GCRMA/LPE	Up	1q31.2	Linkage
ROBO1	Roundabout, axon guidance receptor, homolog 1 (Drosophila)	LPE	Down	3p13	
RORA	RAR-related orphan receptor A	GCRMA/LPE	Down	15q21.3	Linkage
RPS6KA2	Ribosomal protein S6 kinase, 90 kDa, polypeptide 2	GCRMA/LPE	Up	6q27	Linkage

Abbreviations: GCRMA, GC robust multichip analysis; LPE, local pooled error.
[a] Direction of change in affected compared to unaffected sibling.

(Bolstad, Irizarry, Astrand, & Speed, 2003), (3) calculation of expression measures using median polish. Additional normalization was then applied to the summarized data. The local pooled error (LPE) test was then applied to search for differentially expressed genes. The LPE approach is similar to the Significance Analysis of Microarrays (SAM) method (Tusher, Tibshirani, & Chu, 2001) and the B-statistic (Lonnstedt & Speed, 2002). To account for the multiple testing issue inherent to analysis of data from microarray experiments, Bonferroni correction was used to control for the family wise error rate equal to 0.05. Our results were further confirmed using a second summarizing method, which is a variation of the RMA called GCRMA (Wu & Irizarry, 2004). Analysis was completed using S + arrayanalyzer 2.0 from Insightful (http://www.insightful.com).

Ingenuity Pathway Software (Ingenuity Systems, Inc., Redwood City, CA) was used to analyze gene function and pathways/networks of significant microarray genes using probe names and fold differences between affected siblings compared to their unaffected siblings.

2.4. Real-time quantitative polymerase chain reaction (qRT-PCR)

Total RNA was isolated from 32 index patients and 35 unaffected control samples that were part of the extremely discordant sibpair cohort analyzed in both the gene expression and linkage studies, using Trizol (Invitrogen, Carlsbad, CA). Eighty nanograms of total RNA was reverse transcribed using SuperScript III First-Strand Synthesis SuperMix (Invitrogen). One microliter of cDNA sample, and 0.5 μl probe were used in a 10 μl PCR reaction, and five replicates were performed for each probe using Taqman Gene Expression Master Mix (Applied Biosystems, Foster City, CA). Premade Applied Biosystems (ABI) probes labeled with FAM were used to amplify *RORA* (ABI, hs00933986_m1, hs01387931_m1, hs01387932_m1) and *β-actin* (ABI, hs99999903_m1). Reactions were quantified using an ABI 7500 Real Time PCR instrument and analyzed with accompanying software. Relative expression levels were determined by normalizing cycle threshold values for each primer to the amount of *β-actin* expressed (1000/2^(Ct-gene-Ct-: *β-actin*). Relative fold change was calculated from normalized values. Significant expression differences were assessed by the student's paired *T*-Test.

2.5. Genotyping of microsatellite markers

For the genotyping of microsatellite markers, the Sequenom iPLEX system technology, and direct sequencing protocols, leukocyte DNA was either purified by using standard phenol–chloroform or DNAzol (Invitrogen) extraction protocols. Using 133 extremely discordant sibling pairs, we analyzed 18 highly heterozygous microsatellite markers spanning 34 megabases of the 15q21-22 region (Supplementary Table 2). These markers included several that were in the vicinity of *RORA*. All markers were fluorescently labeled with either 5-carboxyfluorescein or 6-carboxyfluorescein on the 5′ end of the reverse primer and an additional sequence of CTGTCTT was added to the 5′ end of the forward primer. PCR was used to amplify genomic DNA fragments from 20 ng of leukocyte DNA in a solution of 10 × PCR buffer containing 25 mmol/L of $MgCl_2$; 0.2 mmol/L each of deoxyadenosine triphosphate, deoxythymidine triphosphate, deoxyguanosine triphosphate, and deoxycytidine triphosphate; and 0.5 U of Taq DNA polymerase (USB Corporation, Cleveland, OH). PCR cycling conditions were as follows, 95 °C for 5 min, followed by 35 cycles of 54–60 °C (specific to primer pair) for 30 s, 72 °C for 30 s, and 95 °C for 30 s, with a final annealing at 54–60 °C (specific to primer pair) for 1.5 min and extension of 72 °C for 5 min. Polymerase chain reaction products were diluted 1:20 for markers labeled with FAM and 1:10 for markers labeled with HEX. Samples were pooled according to product size and denatured before being genotyped on the ABI 3730 × l DNA Analyzer (Applied Biosystems). Data were then analyzed using ABI's Genemapper 3.7 software, which interrogates the quality of the size standard and makes the appropriate genotype calls based on size. For quality control purposes, all genotypes were then evaluated manually.

For linkage analysis of the 18 microsatellite markers, identity-by-state (IBS) scores were calculated from the number of alleles (0, 1 or 2) shared between each pair, the index and the discordant sibling, for each of the 18 markers. Using heterozygosities for each marker obtained from Map-O-Mat (http://compgen.rutgers.edu/mapomat/),

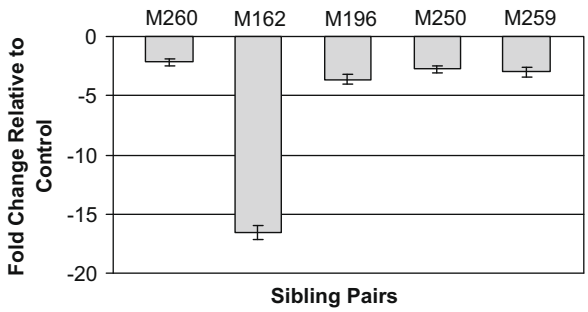

Fig. 2. Quantitative real time-PCR analysis reveals reduction of *RORA* expression in AMD patients of the extremely discordant sibling pairs. The graph represents data from five families depicting reduction of *RORA* expression in AMD patients relative to their respective unaffected sibling pair; $p < 0.04$. Each bar is labeled with the family identification number and error bars indicating standard error of the mean.

the expected IBS (null hypothesis of no linkage) was calculated and then compared with the observed IBS values. A goodness of fit test was applied to assess the significance of the difference between the observed and expected distribution. This method has been used previously for linkage analysis in sibling pairs (DeAngelis et al., 2008).

2.6. Genotyping analysis

RORA is located on chromosome 15q and spans approximately 730 kilobases. We analyzed SNP location in terms of the largest of four transcripts, which encodes 12 exons as shown in ENSEMBL (*RORA-001*: ENST00000335670) (http://www.ensembl.org/index.html). Single nucleotide polymorphisms (SNPs) were chosen for analysis at approximately every 5000 base pairs (when variation information was available) in an effort to represent the entire variation within the gene (Supplementary Table 2). Based on the location of SNPs and haplotypes found to be significantly associated with neovascular AMD, 11 TagSNPs were chosen for genotyping using the HapMap (http://www.hapmap.org/) and meeting the following criteria: (1) a minor allele frequency greater than 10% and (2) an r^2 value that was at least 0.8 (Supplementary Table 2).

Multiplex PCR assays were designed using Sequenom SpectroDESIGNER software (version 3.0.0.3) (Sequenom, San Diego,

Table 2
Chromosome 15 microsatellite markers.

D15S1015	# of pairs	D15S125	# of pairs	D15S974	# of pairs	D15S1036	# of pairs	D15S527	# of pairs	D15S643	# of pairs
# of 0's	20	# of 0's	12	# of 0's	20	# of 0's	15	# of 0's	29	# of 0's	25
# of 1's	56	# of 1's	56	# of 1's	68	# of 1's	71	# of 1's	58	# of 1's	69
# of 2's	52	# of 2's	49	# of 2's	38	# of 2's	40	# of 2's	33	# of 2's	37
Total	128	Total	117	Total	126	Total	126	Total	120	Total	131
# of na	5	# of na	16	# of na	7	# of na	7	# of na	13	# of na	2
h	0.905	*h*	0.793	*h*	0.969	*h*	0.848	*h*	0.88	*h*	0.872
Chi-sq	7.182	Chi-sq	3.180	Chi-sq	4.117	Chi-sq	4.115	Chi-sq	2.024	Chi-sq	0.848
p-Value	0.0276	*p*-Value	0.2039	*p*-Value	0.1276	*p*-Value	0.1278	*p*-Value	0.3635	*p*-Value	0.6543
D15S117	# of pairs	D15S209	# of pairs	D15S143	# of pairs	D15S659	# of pairs	D15S214	# of pairs	D15S1012	# of pairs
# of 0's	11	# of 0's	12	# of 0's	11	# of 0's	23	# of 0's	5	# of 0's	13
# of 1's	73	# of 1's	75	# of 1's	55	# of 1's	61	# of 1's	59	# of 1's	71
# of 2's	35	# of 2's	43	# of 2's	64	# of 2's	40	# of 2's	64	# of 2's	46
Total	119	Total	130	Total	130	Total	124	Total	128	Total	130
# of na	14	# of na	3	# of na	3	# of na	9	# of na	5	# of na	3
h	0.829	*h*	0.78	*h*	0.65	*h*	0.85	*h*	0.43	*h*	0.74
Chi-sq	9.208	Chi-sq	6.446	Chi-sq	1.000	Chi-sq	0.043	Chi-sq	8.721	Chi-sq	3.683
p-Value	0.0100	*p*-Value	0.0398	*p*-Value	0.6065	*p*-Value	0.9787	*p*-Value	0.0128	*p*-Value	0.1586
D15S1042	# of pairs	D15S118	# of pairs	D15S971	# of pairs	D15S1232	# of pairs	D15S1040	# of pairs	D15S1007	# of pairs
# of 0's	21	# of 0's	15	# of 0's	17	# of 0's	27	# of 0's	15	# of 0's	25
# of 1's	56	# of 1's	68	# of 1's	65	# of 1's	57	# of 1's	60	# of 1's	68
# of 2's	49	# of 2's	43	# of 2's	43	# of 2's	35	# of 2's	37	# of 2's	35
Total	126	Total	126	Total	125	Total	119	Total	112	Total	128
# of na	7	# of na	7	# of na	8	# of na	14	# of na	21	# of na	5
h	0.83	*h*	0.749	*h*	0.81	*h*	0.87	*h*	0.77	*h*	0.87
Chi-sq	1.263	Chi-sq	2.571	Chi-sq	1.010	Chi-sq	1.165	Chi-sq	1.747	Chi-sq	1.276
p-Value	0.5319	*p*-Value	0.2765	*p*-Value	0.6036	*p*-Value	0.5584	*p*-Value	0.4175	*p*-Value	0.5283

Abbreviations: #, number; na, non-applicable; *h*, heterozygocity.

Table 3
FBAT analysis of *RORA* SNPs in the extremely discordant sibling pair cohort (n = 150).

Marker	Allele	Freq.	Additive model			Dominant model			Recessive model		
			No. of informative families	*Z* score	*p*-Value	No. of informative families	*Z* score	*p*-Value	No. of informative families	*Z* score	*p*-Value
rs12916023	C	0.541	65	1.709	0.0874	29	0.557	0.5775	40	1.897	0.0578
rs4583176	T	0.229	39	0.926	0.3545	33	1.219	0.2230	7	−0.378	0.7055
rs730754	G	0.377	65	−0.798	0.4250	46	−1.180	0.2382	23	0.209	0.8348
rs8034864	A	0.216	44	0.729	0.4658	39	0.801	0.4233	6	0.000	1.0000
rs975501	G	0.390	65	−1.162	0.2450	43	−1.372	0.1699	25	−0.200	0.8415
rs12900948	G	0.389	67	−1.013	0.3113	45	−1.043	0.2967	26	−0.392	0.6949
rs782925	A	0.194	33	−1.219	0.2230	30	−1.826	0.0679	<4	n/a	n/a
rs7177611	T	0.280	47	−0.762	0.4461	40	−0.949	0.3428	12	0.000	1.0000
rs1403737	T	0.258	49	0.122	0.9028	41	0.781	0.4349	14	−1.069	0.2850
rs12591914	T	0.303	54	0.516	0.6056	39	2.082	0.0374	17	−2.183	0.0290
rs16943429	G	0.168	38	−0.302	0.7630	35	−0.845	0.3980	5	1.342	0.1797
rs7495128	A	0.186	40	0.295	0.7681	35	−0.169	0.8658	7	1.134	0.2568
rs2414687	T	0.307	45	−0.140	0.8886	39	0.480	0.6310	8	−1.414	0.1573
rs17237514	G	0.156	42	1.543	0.1228	38	1.298	0.1944	4	1.000	0.3173
rs4335725	A	0.366	53	−1.364	0.1724	38	0.324	0.7456	19	−2.982	0.0029
rs17270640	G	0.290	50	1.069	0.2850	39	1.441	0.1495	13	−0.277	0.7815
rs11071570	C	0.347	51	1.033	0.3017	37	0.822	0.4111	17	0.728	0.4669
rs6494231	A	0.399	55	−1.750	0.0801	33	−1.219	0.2230	25	−1.400	0.1615

Abbreviations: No., Number; Freq., Frequency.

CA) by inputting sequence containing the SNP site and 100 base pairs of flanking sequence on either side of the SNP. Briefly, 10 ng genomic DNA was amplified in a 5 μl reaction containing 1 × HotStar Taq PCR buffer (Qiagen, Valencia, CA), 1.625 mM $MgCl_2$, 500 μm each dNTP, 100 nM each PCR primer, 0.5 U HotStar Taq (Qiagen). The reaction was incubated at 94 °C for 15 min followed by 45 cycles of 94 °C for 20 s, 56 °C for 30 s, 72 °C for 1 min, followed by 3 min at 72 °C. Excess dNTPs were removed from the reaction by incubation with 0.3 U shrimp alkaline phosphatase (USB Corporation) at 37 °C for 40 min followed by a 5 min incubation at 85 °C to deactivate the enzyme. Single primer extension over the SNP was carried out in a final concentration of between 0.625 μm and 1.5 μm for each extension primer (depending on the mass of the probe), iPLEX termination mix (Sequenom), and 1.35 U iPLEX enzyme (Sequenom), and cycled using a two-step 200 short cycles program; 94 °C for 30 s followed by 40 cycles of 94 °C for 5 s, 5 cycles of 52 °C for 5 s, and 80 °C for 5 s, then 72 °C for 3 min. The reaction was then desalted by addition of 6 mg cation exchange resin followed by mixing and centrifugation to settle the contents of the tube. The extension product was then spotted onto a 384 well SpectroCHIP (Sequenom) before being flown in the MALDI-TOF mass spectrometer. Data was collected, real time, using SpectroTYPER Analyzer 3.3.0.15, SpectraAQUIRE 3.3.1.1 and SpectroCALLER 3.3.0.14 (Sequenom). To ensure data quality, genotypes for each subject were also checked manually.

For some replicate samples, direct sequencing was performed. For these reactions, oligonucleotide primers were selected using the Primer3 program (http://primer3.sourceforge.net/) to encompass the SNP and flanking intronic sequences.

All PCR assays were performed using genomic DNA fragments from 20 ng of leukocyte DNA in a solution of 10 × PCR buffer containing 25 mM of $MgCl_2$, 0.2 mM each of dATP, dTTP, dGTP, and dCTP, and 0.5 U of Taq DNA polymerase (USB Corporation). Five molar betaine was added to the reaction mix for rs2414687 (Sigma–Aldrich, St. Louis, MO). The temperatures used during the polymerase chain reaction were as follows: 95 °C for 5 min followed by 35 cycles of 58 °C for 30 s, 72 °C for 30 s and 95 °C for 30 s, with a final annealing at 58 °C for 1.5 min and extension of 72 °C for 5 min. For sequencing reactions, PCR products were digested according to manufacturer's protocol with ExoSAP-IT (USB Corporation) then were subjected to a cycle sequencing reaction using the Big Dye Terminator v 3.1 Cycle Sequencing kit (Applied Biosystems, Foster City, CA) according to manufacturer's protocol. Products were purified with Performa DTR Ultra 96-well plates (Edge Biosystems, Gaithersburg, MD) in order to remove excess dye terminators. Samples were sequenced on an ABI Prism 3100 DNA sequencer (Applied Biosystems). Electropherograms generated from the ABI Prism 3100 were analyzed using the Lasergene DNA and protein analysis software (DNASTAR, Inc., Madison, WI). Electropherograms were read by two independent evaluators without knowledge of the subject's disease status. All patients were sequenced in the forward direction (5′–3′), unless variants or polymorphisms were identified, in which case confirmation was obtained in some cases by sequencing in the reverse direction.

Testing of association between SNPs and AMD in the 196 sibling pairs was done using the family-based association test (FBAT) (http://biosun1.harvard.edu/~fbat/fbat.htm). SNPs were tested for association using the minor allele, as defined by the allele occurring less frequently in the unaffected siblings. Alleles were tested under three genetic models: additive, dominant and recessive. SNPs were only included for analysis in FBAT if the minor allele frequency (MAF) in the affected and unaffected siblings combined was greater than or equal to 5% and the number of informative families was at least four. Linkage disequilibrium (LD) (both r^2 and D') between each of the SNPs was determined using the program Haploview (http://www.broad.mit.edu/mpg/haploview/). Haplotype blocks were constructed in Haploview using the method proposed by Gabriel et al. (2002) Individual haplotypes were inferred and tested for association with AMD using the program FBAT. In order to correct for multiple testing in FBAT, the permutation test was used to examine each of the resulting haplotypes.

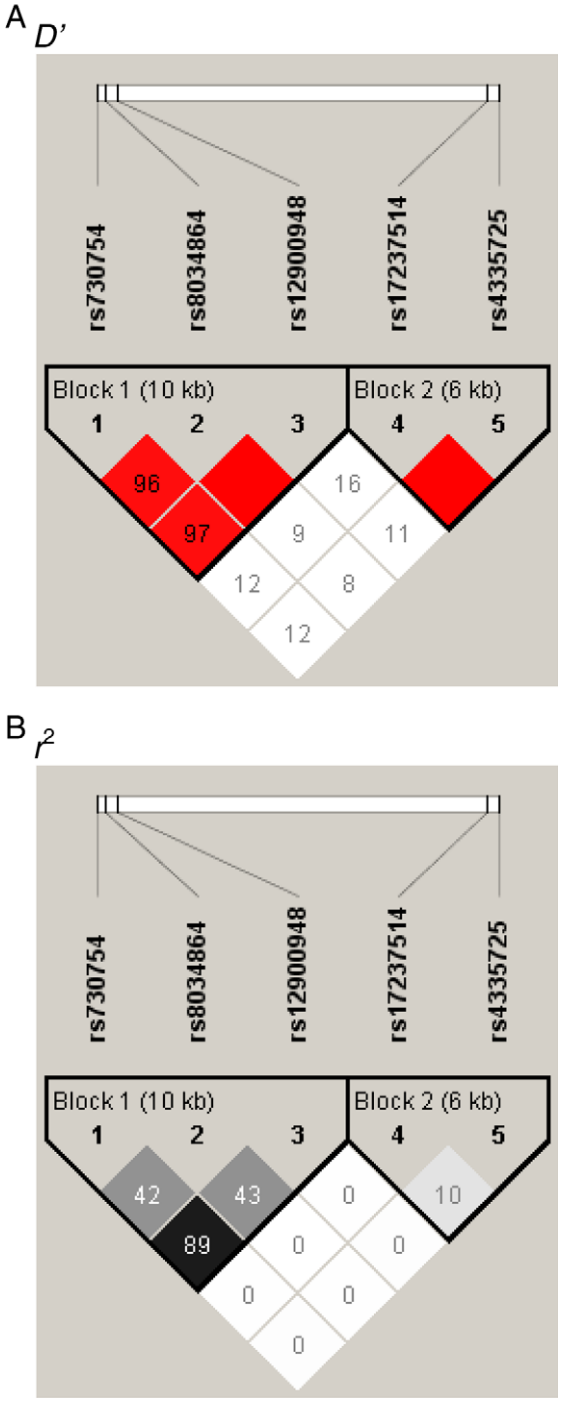

Fig. 3. Linkage disequilibrium plots for the extremely discordant sibling cohort (n = 150 sibling pairs). Haplotype blocks were constructed in Haploview using the method proposed by Gabriel et al. (2002). Boxes were shaded increasingly darker to represent higher percentage of LD and the numbers listed in each square represent the D' (A) and r^2 values (B) unless the box is completely shaded in representing complete LD. Two haplotype blocks were generated for this cohort.

Genotype and allele frequencies for all SNPs identified as significant, either individually or as part of a haplotype, were calculated in affected and separately in unaffected individuals. Deviation from Hardy–Weinberg Equilibrium was tested on each SNP using the chi square test.

Risk factors were controlled for using conditional logistic regression performed using SAS (SAS, version 9.1; SAS Institute Inc., Cary, NC). Included in this analysis were those SNPs identified as significantly associated with neovascular AMD and known risk factors. Known risk factors for the extremely discordant sibling pair cohort included smoking history and the genetic variants *CFH* rs1061170 (Y402H) and *ARMS2/HTRA1* rs10490924/rs11200638 (DeAngelis et al., 2008; Zhang et al., 2008). Conditional logistic regression was also used to test gene–gene interaction between *RORA* SNPs identified as significantly associated with AMD and the *CFH* and the *ARMS2/HTRA1* loci individually. Similarly, conditional logistic regression was used to test gene–environment interaction between *RORA* and smoking.

For replication in the unrelated case-control cohort from Central Greece, single SNP analysis and haplotype analysis was performed using unconditional logistic regression (UCLR) in SAS (SAS, version 9.1; SAS Institute Inc., Cary, NC) under the same three genetic models: additive, dominant, and recessive. Linkage disequilibrium was also tested using Haploview.

2.7. Expression quantitative trait loci analysis

Using the publicly available expression quantitative trait loci (eQTL) database mRNA by SNP Browser v 1.0.1 (Dixon et al., 2007; Moffatt et al., 2007; Shimada et al., 2009), we investigated the association between eQTLs and the *RORA* SNPs that were identified as significant either individually or as part of a haplotype.

3. Results

3.1. Patient population

We recruited a total of 196 sibling pairs, 150 of which were extremely discordant sibling pairs (one sibling with neovascular AMD and one normal sibling – AREDS category 1 or less) and the remaining 46 were discordant, meaning one sibling had neovascular AMD and the other sibling had early dry, AMD (AREDS category 2) (Supplementary Table 1). The mean ± SD age of the affected siblings (neovascular AMD) was 72.1 ± 8.0 years (age range, 49.0–92.0 years), the age of the mildly affected siblings (dry AMD) was 77.4 ± 7.0 years (age range, 58.2–89.1 years), and the age of the unaffected siblings was 76.4 ± 7.8 years (age range, 50.3–94.3 years). Forty-one percent of the unaffected siblings, 30% of the dry AMD siblings and 43% of the matching affected siblings were male. All participants were white and mostly of European descent.

The cohort from Central Greece consisted of a total of 344 patients: 121 normal controls, 84 early dry patients (AREDS categories 2 and 3), and 139 neovascular patients (Supplementary Table 1). The mean ± SD age of the affected subjects (neovascular AMD) was 76.2 ± 7.4 years (age range, 49.0–94.0 years), the age of the mildly affected subjects (dry AMD) was 74.5 ± 7.8 years (age range, 52.0–91.0 years), and the age of the unaffected subjects was 73.5 ± 7.3 years (age range, 48.0–88.0 years). Fifty-one percent of the unaffected subjects, 44% of the AREDS category 2 and AREDS category 3 AMD subjects and 45% of the neovascular subjects were male. All participants were white and from Central Greece.

3.2. Gene expression analysis

We compared microarray data from nine extremely discordant sibling pairs that had been matched for smoking history, age, sex, cardiovascular disease history, body mass index, hypertension, and hypercholesterolemia. To create a short list of candidate genes for further study, we used Ingenuity Pathway Analysis (IPA) software to investigate known functions and pathways of statistically significant genes that were identified by either LPE or GCRMA and had at least a 2-fold difference in expression levels. To focus our studies, we concentrated on the IPA-generated network that encompassed the greatest number of genes (Fig. 1 and Supplementary Table 3). Within this network, the individual genes that were identified by LPE and GCRMA are chemokine (C-X-C motif) ligand 13 (*CXCL13*), interleukin 1 alpha (*IL1A*), matrix metallopeptidase 7 (*MMP7*), plakophilin 2 (*PKP2*), phospholipase A2 group IVA (*PLA2-G4A*), NLR family, pyrin domain containing 2 (*NLRP2*), regulator of G-protein signaling 13 (*RGS13*), roundabout, axon guidance receptor, homolog 1 (Drosophila) (*ROBO1*), RAR-related orphan receptor

Table 4
FBAT haplotype analysis of *RORA* in the extremely discordant sibling pair cohort (n = 150 pairs).

Gabriel rule Order	rs730754	rs8034864	rs12900948	Freq.	No. of informative families	p-Value
Block 1 – additive model						
*h*1	A	C	A	0.617	74	0.3637
*h*2	G	A	G	0.199	41	0.2652
*h*3	G	C	G	0.159	49	0.0128
Estimated haplotypes with allele frequency greater than 0.05 were listed and tested for association. When considering all possible haplotypes together, the resulting p-value from 15,606 permutations was 0.0309.						
Block 1 – dominant model						
*h*1	A	C	A	0.617	35	0.9795
*h*2	G	A	G	0.199	36	0.2073
*h*3	G	C	G	0.159	44	0.0062
Estimated haplotypes with allele frequency greater than 0.05 were listed and tested for association. When considering all possible haplotypes together, the resulting p-value from 32,189 permutations was 0.0212.						

Order	rs17237514	rs4335725	Freq.	No. of informative families	p-Value
Block 4 – recessive model					
*h*1	A	G	0.495	31	0.2142
*h*2	A	A	0.359	18	0.0008
*h*3	G	G	0.143	4	0.3745
Estimated haplotypes with allele frequency greater than 0.05 were listed and tested for association. When considering all possible haplotypes together, the resulting p-value from 100,000 permutations was 0.0018.					

Abbreviations: No., Number; Freq., Frequency.

Table 5
Genotype and allele frequencies.

RORA		Neovascular		Unaffected	
		Frequency (%)	No.	Frequency (%)	No.
Extremely discordant sibling pair cohort					
rs730754	Genotype AA	42.18	62	35.62	52
	Genotype GA	43.54	64	50.68	74
	Genotype GG	14.29	21	13.70	20
	Total		147		146
	Allele				
	A	63.95	188	60.96	178
	G	36.05	106	39.04	114
	Total		294		292
rs8034864	Genotype CC	59.18	87	63.01	92
	Genotype AC	36.73	54	32.88	48
	Genotype AA	4.08	6	4.11	6
	Total		147		146
	Allele				
	C	77.55	228	79.45	232
	A	22.45	66	20.55	60
	Total		294		292
rs12900948	Genotype AA	39.86	59	33.56	49
	Genotype GA	46.62	69	51.37	75
	Genotype GG	13.51	20	15.07	22
	Total		148		146
	Allele				
	A	63.18	187	59.25	173
	G	36.82	109	40.75	119
	Total		296		292
rs17237514	Genotype AA	67.81	99	73.47	108
	Genotype GA	29.45	43	25.17	37
	Genotype GG	2.74	4	1.36	2
	Total		146		147
	Allele				
	A	82.53	241	86.05	253
	G	17.47	51	13.95	41
	Total		292		294
rs4335725	Genotype GG	40.14	59	40.69	59
	Genotype AG	51.02	75	41.38	60
	Genotype AA	8.84	13	17.93	26
	Total		147		145
	Allele				
	G	65.65	193	61.38	178
	A	34.35	101	38.62	112
	Total		294		290

RORA		Neovascular		AREDS cat. 2	
		Frequency (%)	No.	Frequency (%)	No.
Discordant sibling pair cohort					
rs730754	Genotype AA	40.00	18	51.11	23
	Genotype GA	48.89	22	26.67	12
	Genotype GG	11.11	5	22.22	10
	Total		45		45
	Allele				
	A	64.44	58	64.44	58
	G	35.56	32	35.56	32
	Total		90		90
rs8034864	Genotype CC	67.39	31	71.11	32
	Genotype AC	26.09	12	22.22	10
	Genotype AA	6.52	3	6.67	3
	Total		46		45
	Allele				
	C	80.43	74	82.22	74
	A	19.57	18	17.78	16
	Total		92		90
rs12900948	Genotype AA	39.13	18	44.44	20
	Genotype GA	50.00	23	28.89	13
	Genotype GG	10.87	5	26.67	12
	Total		46		45
	Allele				
	A	64.13	59	58.89	53
	G	35.87	33	41.11	37

(*continued on next page*)

Table 5 (*continued*)

RORA		Neovascular		Unaffected	
		Frequency (%)	No.	Frequency (%)	No.
	Total		92		90
rs17237514	Genotype AA	60.00	27	66.67	28
	Genotype GA	33.33	15	28.57	12
	Genotype GG	6.67	3	4.76	2
	Total		45		42
	Allele				
	A	76.67	69	80.95	68
	G	23.33	21	19.05	16
	Total		90		84
rs4335725	Genotype GG	50.00	23	51.11	23
	Genotype AG	45.65	21	46.67	21
	Genotype AA	4.35	2	2.22	1
	Total		46		45
	Allele				
	G	72.83	67	74.44	67
	A	27.17	25	25.56	23
	Total		92		90

RORA		Neovascular AMD		Dry AMD		Normal	
		Frequency (%)	No.	Frequency (%)	No.	Frequency (%)	No.
Central Greece cohort							
rs730754	Genotype AA	20.49	25	35.71	30	33.62	39
	Genotype GA	59.84	73	39.29	33	44.83	52
	Genotype GG	19.67	24	25.00	21	21.55	25
	Total		122		84		116
	Allele						
	A	50.41	123	55.36	93	56.03	130
	G	49.59	121	44.64	75	43.97	102
	Total		244		168		232
rs8034864	Genotype CC	45.08	55	60.71	51	51.24	62
	Genotype AC	49.18	60	28.57	24	42.98	52
	Genotype AA	5.74	7	10.71	9	5.79	7
	Total		122		84		121
	Allele						
	C	69.67	170	75.00	126	72.73	176
	A	30.33	74	25.00	42	27.27	66
	Total		244		168		242
rs12900948	Genotype AA	9.91	11	29.49	23	30.70	35
	Genotype GA	70.27	78	38.46	30	45.61	52
	Genotype GG	19.82	22	32.05	25	23.68	27
	Total		111		78		114
	Allele						
	A	45.05	100	48.72	76	53.51	122
	G	54.95	122	51.28	80	46.49	106
	Total		222		156		228
rs17237514	Genotype AA	65.87	83	68.67	57	73.33	88
	Genotype GA	33.33	42	27.71	23	25.83	31
	Genotype GG	0.79	1	3.61	3	0.83	1
	Total		126		83		120
	Allele						
	A	82.54	208	82.53	137	86.25	207
	G	17.46	44	17.47	29	13.75	33
	Total		252		166		240
rs4335725	Genotype GG	56.35	71	60.71	51	52.89	64
	Genotype AG	34.92	44	33.33	28	39.67	48
	Genotype AA	8.73	11	5.95	5	7.44	9
	Total		126		84		121
	Allele						
	G	73.81	186	77.38	130	72.73	176
	A	26.19	66	22.62	38	27.27	66
	Total		252		168		242

A (*RORA*), ribosomal protein S6 kinase, 90 kDa, polypeptide 2 (*RPS6KA2*) (Table 1). This set of genes was simultaneously analyzed with linkage data previously obtained from our laboratory to investigate genomic convergence (Table 1).

Of these genes, *RORA* was selected for further study due to its anti-angiogenic properties (Boukhtouche et al., 2004; Chauvet, Bois-Joyeux, Berra, Pouyssegur, & Danan, 2004; Chauvet et al., 2005), the statistically different expression between affected patients compared to their unaffected siblings, and linkage data (see Section 3.3) demonstrating an association of the 15q region with neovascular AMD. Specifically, 4 *RORA* probes were identified as significantly altered in AMD *vs.* control samples. Three of these

probes showed decreased expression in AMD patients (p-value ranged from 10^{-3} to 10^{-9} after Bonferonni correction) while 1 probe showed increased expression in affected patients ($p = 10^{-4}$ after Bonferonni correction).

In order to confirm the results of the microarray studies, qRT-PCR analysis was performed on RNA from neovascular AMD patients ($n = 32$) and their unaffected control siblings ($n = 35$), which included RNA from seven of the nine original pairs used for the gene expression microarray analysis. The 3 RNA probes used showed a trend of decreased *RORA* expression in this cohort (>1.5-fold; data not shown). Specifically, five of the families showed statistically significant reduction in *RORA* gene expression ranging from 2-fold reduction to as high as 16-fold reduction in an AMD patient compared to their respective sibpair, $p < 0.04$ (Fig. 2).

3.3. Linkage analysis using microsatellite markers

Calculation of identity-by-state scores from the genotyping results of 18 highly heterozygous microsatellite markers in the 15q region identified three markers, D15S1015, D15S209, and D15S214, that were modestly associated with neovascular AMD ($p < 0.05$) (Table 2). The most significantly associated marker, D15S117 ($p = 0.01$), is located approximately 2 megabases from the gene end (*RORA*: ENSG00000069667) (Supplementary Table 2).

3.4. Analysis of RORA SNPs and haplotypes in the extremely discordant sibling pair cohort

In total, we identified 92 SNPs in the *RORA* gene demonstrating variation in our extremely discordant sibling pair cohort (discovery cohort) ($n = 150$ pairs; 300 subjects) (for SNPs and location refer to Supplementary Table 2). No significant deviations from Hardy–Weinberg equilibrium for any of the variants studied were observed in either affected or unaffected siblings, suggesting unlikely contamination of our dataset. Single SNP analysis using FBAT in our discovery cohort identified rs12591914 and rs4335725, variants located within intron 1 of the *RORA-001* transcript (ENST00000335670), as modestly ($p = 0.029$) and significantly ($p = 0.0029$) associated under a recessive model respectively (Table 3). The *RORA* SNP rs4335725 remained significant ($p \leqslant 0.007$) after controlling for the following factors: *CFH* rs1061170 (Y402H), *ARMS2/HTRA1* rs10490924/rs11200638, and smoking history in a multiple logistic regression model; however, the rs12591914 SNP did not remain significant (data not shown).

Haploview, using haplotype blocks defined by the Gabriel rule (Gabriel et al., 2002), demonstrated that there were 13 haplotype blocks spanning the more than 700,000 base pairs covered by genotyping (Supplementary Figs. 1 and 2 and Table 2). Of the 13 haplotype blocks, two blocks, both located in intron 1 and comprising three haplotypes, were shown to be significantly associated with neovascular AMD risk in FBAT [*h*3 in block 1 (GCG) under both additive ($p = 0.0128$) and dominant ($p = 0.0062$) genetic models, as well as *h*2 in block 4 (AA) under a recessive ($p = 0.0008$) genetic model (Fig. 3 and Table 4)]. The overall permutations for the first haplotype in block 1 under both an additive and a dominant model was $p = 0.03$ and $p = 0.02$, respectively. The overall permutation for the second haplotype block was $p = 0.0018$ under a recessive model. Conservation analysis showed that the SNPs comprising these two haplotypes blocks (rs730754, rs8034864, rs12900948, rs17237514 and rs4335725) (Fig. 3) are all well conserved in both rat and mouse. Genotype and allele frequencies for these 5 SNPs are given in Table 5. Based on these findings, we chose 11 tagging SNPs within intron 1 to further capture variation and refine this region, which is approximately 550 kilobases, for further study. Statistical analysis using FBAT showed that none of the *RORA* intron 1 tagging SNPs were informative individually or as part of a haplotype as they did not remain significantly associated with neovascular AMD after correction for multiple testing.

3.5. Analysis of RORA SNPs and haplotypes in the AREDS category 2 discordant sibling pair cohort

The 5 SNPs that comprised the two haplotype blocks containing significant haplotypes in the discovery cohort (rs730754, rs8034864, rs12900948, for block 1 and rs17237514 and rs4335725 for block 4) were tested for association in the AREDS category 2 discordant sibling pair cohort where the index patient had the neovascular form of AMD and the matched sibling had the early/dry form of AMD (AREDS category 2). Single SNP analysis of these five SNPs using FBAT showed that one SNP, rs12900948, was modestly associated with decreased risk of developing neovascular AMD under a recessive genetic model ($p = 0.034$) (Table 6). This SNP, like rs4335725, is also located in intron 1 of the *RORA-001* transcript (ENST00000335670) and is also well conserved.

Haploview was used to create LD plots for this cohort (Fig. 4). Like the extremely discordant sibling pairs, applying the Gabriel rule demonstrated that block 1 containing SNPs rs730754, rs8034864 and rs12900948 was the same between both sibling pair cohorts studied (Figs. 3 and 4). However, the second haplotype block identified in the initial discovery cohort of extremely discordant sibling pairs was not found in the AREDS category 2 discordant sibling pair cohort. This may be due to the much smaller sample size analyzed ($n = 46$ discordant sibling pairs). FBAT analysis of these two haplotype blocks in the AREDS category 2 discordant sibling pair cohort demonstrated that one haplotype (ACA) within this block was modestly associated with neovascular AMD risk ($p = 0.0492$). However, after permutation testing this finding was no longer significant ($p = 0.114$) (Supplementary Table 4).

3.6. Analysis of RORA SNPs and haplotypes in the Greek cohort

The SNPs that comprised the significant haplotypes (rs730754, rs8034864, rs12900948, for block 1 and rs17237514 and

Table 6
FBAT analysis of *RORA* SNPs in the AREDS category 2 discordant sibling pair cohort ($n = 46$ pairs).

Marker	Allele	Freq.	Additive model			Dominant model			Recessive model		
			No. of informative families	*Z* score	*p*-Value	No. of informative families	*Z* score	*p*-Value	No. of informative families	*Z* score	*p*-Value
rs730754	G	0.348	14	0.243	0.8084	7	1.890	0.0588	8	−2.000	0.1573
rs8034864	A	0.183	9	0.333	0.7389	7	0.378	0.7055	<4	n/a	n/a
rs12900948	G	0.378	13	−1.000	0.3173	6	0.816	0.4142	8	−3.000	0.0339
rs17237514	G	0.215	9	−0.577	0.5637	9	−0.333	0.7389	<4	n/a	n/a
rs4335725	A	0.261	16	0.500	0.6171	13	0.277	0.7815	<4	n/a	n/a

Abbreviations: No., Number.

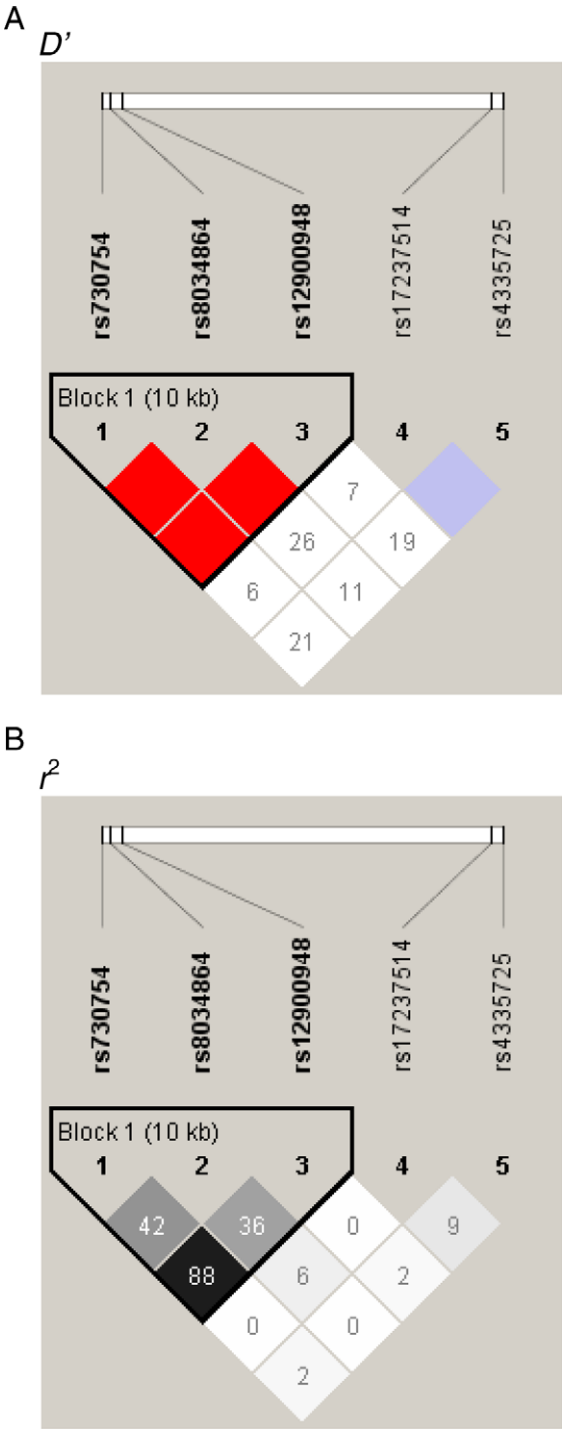

Fig. 4. Linkage disequilibrium plots for the AREDS 2 discordant sibling cohort ($n = 46$ sibling pairs). Haplotype blocks were constructed in Haploview using the method proposed by Gabriel et al. (2002). Boxes were shaded increasingly darker to represent higher percentage of LD and the numbers listed in each square represent the D' (A) and r^2 values (B) unless the box is completely shaded in representing complete LD. A single haplotype block was generated for this cohort.

rs4335725 for block 4) in the discovery cohort were genotyped and tested for association in the Greek population ($n = 344$) using unconditional logistic regression. This analysis showed that only rs12900948 was significantly associated with neovascular AMD when comparing neovascular AMD patients to normal patients and separately to patients with early and intermediate dry AMD (AREDS categories 2 and 3) under either a dominant or recessive model (Table 7). Specifically, the G allele (which is the minor allele for both family-based cohorts but the major allele for the Greek cohort) of rs12900948 increased risk of neovascular AMD in the unrelated case-control cohort by 4-fold and 3.8-fold when compared to normal patients and separately to patients with dry AMD respectively (OR: 4.028; 95% C.I.: 1.924, 8.433; $p = 0.0002$ and OR: 3.802; 95% C.I.: 1.725, 8.379; $p = 0.0009$). When we compared the G allele of rs12900948 in normal controls (AREDS category 1 or less) to all subtypes of AMD in this unrelated case-control cohort, this finding was much more modestly associated (OR: 2.020; 95% C.I.: 1.172, 3.480; $p = 0.0113$).

Haploview analysis using the Gabriel rule showed that there was a single haplotype block in the Greek unrelated case-control cohort (Fig. 5). This haplotype block, containing SNPs rs730754, rs8034864, rs12900948, was common to the cohort from Central Greece and both family-based cohorts studied (Figs. 3–5). While SNPs rs17237514 and rs4335725 comprised a haplotype block for the initial discovery family-based cohort of extremely discordant sibling pairs, these SNPs did not comprise a second block (block 4) in the unrelated case-control cohort from Central Greece. Nonetheless, both blocks initially identified in the discovery cohort were tested in unconditional logistic regression in the unrelated case-control cohort. In the Greek population, the single haplotype block identified by the Gabriel rule in Haploview was significantly associated with AMD risk. Specifically, when either comparing neovascular patients to unaffected patients or separately, to dry patients, the *h*2 (GAG) haplotype was significantly associated with AMD risk under a dominant model (OR: 1.470; 95% C.I.: 1.148,1.882; $p = 0.0022$ and OR: 1.584; 95% C.I.:1.204,2.085; $p = 0.0010$, respectively) (Table 8). A second, more modestly associated haplotype, *h*3 (GCG), in this same block (block 1), was also identified under a dominant model for both the comparison of neovascular patients to normal subjects and separately for neovascular patients compared to subjects with dry AMD (AREDS categories 2 and 3) (OR: 1.639; 95% C.I.: 1.032,2.603; $p = 0.0363$ and OR: 1.718; 95% C.I.:1.01,2.905; $p = 0.0432$, respectively).

3.7. Interaction of RORA SNPs with CFH and ARMS2/HTRA1

Using conditional logistic regression, interaction was tested between *RORA* and *CFH*, *ARMS2/HTRA1* and smoking in the discovery cohort of 150 extremely discordant sibling pairs. No significant interaction was found between *RORA* and *CFH* and separately between *RORA* and smoking history. A significant interaction was found between the *RORA* SNP rs12900948 and the *ARMS2/HTRA1* SNPs rs10490924, rs11200638, and rs1049331 ($p = 0.0044$, 0.0044, and 0.0038 respectively). Based on this data, we incorporated *HTRA1* into the network pathway analysis that included *RORA* using IPA's "Path Designer" function to explore a hypothetical molecular means of interaction (Fig. 6). The addition of *HTRA1* introduced the following genes: bone morphogenetic protein 4 (*BMP4*), family with sequence similarity 46, member A (*FAM46A*), fibronectin 1 (*FN1*), growth differentiation factor 5 (*GDF5*), interleukin 13 (*IL13*), matrix metallopeptidase 3 (*MMP3*), matrix metallopeptidase 1 (*MMP1*), serpin peptidase inhibitor, clade A, member 1 (*SERPINA1*), transforming growth factor, beta 2 (*TGFβ2*), transforming growth factor, beta 3 (*TGFβ3*) into the analysis (Supplementary Table 5). *ARMS2* was not included in network analysis as it was not available by IPA's database.

3.8. eQTL analysis

Increasingly, data from GWAS and microarray studies have been analyzed in combination to uncover expression quantitative trait loci (eQTL) that relate specific SNPs to global or tissue specific expression of gene transcripts (Cookson, Liang, Abecasis, Moffatt, &

Table 7
UCLR analysis of *RORA* SNPs in the Greek cohort.

Risk factor	Allele	Additive model		Dominant model		Recessive model	
		Odds ratio (95% C.I.)	*p*-Value	Odds ratio (95% C.I.)	*p*-Value	Odds ratio (95% C.I.)	*p*-Value
All AMD – neo + dry vs. normal							
rs730754	G	1.155 (0.837–1.593)	0.3816	1.391 (0.849–2.278)	0.1905	1.017 (0.586–1.768)	0.9583
rs8034864	A	1.047 (0.729–1.503)	0.8050	0.991 (0.633–1.553)	0.9698	1.371 (0.548–3.434)	0.5001
rs12900948	G	1.345 (0.956–1.894)	0.0891	2.020 (1.172–3.480)	0.0113	1.066 (0.619–1.836)	0.8171
rs17237514	G	1.360 (0.854–2.164)	0.1948	1.355 (0.825–2.227)	0.2303	2.322 (0.257–21.017)	0.4536
rs4335725	A	0.883 (0.622–1.254)	0.4874	0.810 (0.516–1.270)	0.3585	1.026 (0.439–2.399)	0.9523
Neo vs. normal							
rs730754	G	1.271 (0.875–1.846)	0.2072	1.965 (1.095–3.526)	0.0235	0.891 (0.475–1.671)	0.7200
rs8034864	A	1.186 (0.778–1.806)	0.4275	1.280 (0.773–2.119)	0.3377	0.991 (0.337–2.917)	0.9873
rs12900948	G	1.502 (0.996–2.264)	0.0523	4.028 (1.924–8.433)	0.0002	0.797 (0.422–1.504)	0.4830
rs17237514	G	1.381 (0.817–2.335)	0.2272	1.425 (0.824–2.462)	0.2048	0.952 (0.059–15.393)	0.9724
rs4335725	A	0.949 (0.643–1.400)	0.7908	0.870 (0.527–1.436)	0.5856	1.190 (0.475–2.983)	0.7101
Neo vs. dry							
rs730754	G	1.228 (0.822–1.837)	0.3162	2.156 (1.152–4.033)	0.0163	0.735 (0.378–1.430)	0.3640
rs8034864	A	1.310 (0.838–2.048)	0.2369	1.883 (1.070–3.311)	0.0281	0.507 (0.181–1.420)	0.1964
rs12900948	G	1.190 (0.761–1.859)	0.4456	3.802 (1.725–8.379)	0.0009	0.524 (0.269–1.020)	0.0573
rs17237514	G	0.999 (0.584–1.711)	0.9979	1.136 (0.628–2.054)	0.6735	0.213 (0.022–2.087)	0.1843
rs4335725	A	1.197 (0.770–1.862)	0.4247	1.197 (0.683–2.100)	0.5301	1.511 (0.505–4.518)	0.4600

Lathrop, 2009). Using the publicly available eQTL database mRNA by SNP Browser v 1.0.1 (Dixon et al., 2007; Moffatt et al., 2007), we investigated the association of the *RORA* SNPs that comprised our significant haplotypes with eQTLs. Of our 5 SNPs, rs8034864, rs730754, and rs4335725 were present in the database but none were significantly associated with transcript expression according to the method for calculating significance defined by Dixon et al. (Supplementary Table 6). The interaction between the *RORA* SNP rs12900948 and the *ARMS2/HTRA1* SNPs led us to investigate the association of these SNPs, rs10490924, rs11200638, and rs1049331, with transcript expression. Of the ARMS2/HTRA1 SNPs, only rs10490924 was present in the database but was not significantly associated with the expression of any transcripts (Supplementary Table 6).

4. Discussion

In this study, we demonstrate an association between *RORA* and AMD. Using a family-based cohort comprised of extremely discordant sibling pairs, we identified a single *RORA* SNP, rs4335725, and two haplotypes which were significantly associated with neovascular AMD in FBAT. Study of a smaller discordant sibling population [where the index patient had neovascular AMD and the "control sibling" had a mild dry form of AMD (AREDS category 2)] identified a second SNP, rs12900948, as being modestly associated with neovascular AMD. The rs12900948 SNP was part of a haplotype (GCG) that was identified as significantly associated with neovascular AMD risk in the initial discovery cohort of extremely discordant sibling pairs in FBAT. In a separate unrelated case-control cohort from Central Greece, we also identified rs12900948 and two haplotypes containing this SNP (GAG and GCG) as associated with neovascular AMD when compared to either unrelated controls or to unrelated subjects with dry AMD (AREDS categories 2 and 3). Moreover both the rs12900948 and the significant haplotype (rs730754, rs8034864 and rs12900948) that contained this SNP were validated prospectively in nested case-control cohorts from the Nurses' Health Study and the Health Professionals Follow-up Study (D. Schaumberg et al., personal communication).

It is interesting to note that rs12900948 was significant when comparing neovascular patients to patients with the dry form of AMD in both the family-based cohort and in the unrelated case-control cohorts from Central Greece. This may indicate that the risk associated with rs129000948, or as yet to be discovered variants in LD with rs129000948, may specifically relate to the development of neovascular/advanced AMD.

The significant *RORA* variants and haplotypes associated with neovascular AMD in both the family-based and unrelated case-control cohorts occur within the first intron of the *RORA-001* transcript (ENST00000335670), a region that is well conserved across species, including mouse and rat. Although there is no apparent functional change, it is interesting to speculate that these or other undiscovered variations in intron 1, such as an insertion or deletion resulting in a change in copy number, may change the structure of the transcript and/or the sequence of unidentified modifying elements (e.g. silencers or enhancers) (Hastings, Lupski, Rosenberg, & Ira, 2009; Lupski, 2007) In turn, these variations could theoretically influence gene expression by altering modifying elements, increasing/decreasing RNA transcript stability, or affecting splicing with a resultant change in isoform expression (Hollams, Giles, Thomson, & Leedman, 2002; Maddox et al., 2008; Margulies & Birney, 2008).

However, it is most likely that the causal sequence change(s) in this region has yet to be identified as suggested by analysis of the significant haplotypes. For example, the haplotype containing SNP rs4335725 was more significantly associated with risk of neovascular AMD than rs4335725 alone, suggesting that the causal variant(s) is likely in LD with this region. Additionally, SNP rs12900948 was significantly associated with neovascular AMD risk in the discovery cohort as part of a haplotype but not individually. To begin to resolve these questions, further sequencing of the exons and the acceptor/donor splice sites adjacent to this region as well as functionally evaluating each sequence variant for its influence on gene expression is currently being conducted.

Included in our study is expression analysis of *RORA* in lymphoblastoid cell lines. Initial microarray data showed significant changes in both directions, with the majority of probes indicating decreased expression in affected patients. When evaluating an expanded population ($n = 67$) with qRT-PCR to clarify and validate the finding of the gene expression microarray analysis, we observed an overall trend of decreased *RORA* expression in affected patients compared to their unaffected siblings, with statistically significant reduction in *RORA* gene expression in five of these families. A limitation of these expression studies is that they did not assay the individual expression of each of the four *RORA* isoforms, which have been shown to have both temporal- and tissue specific

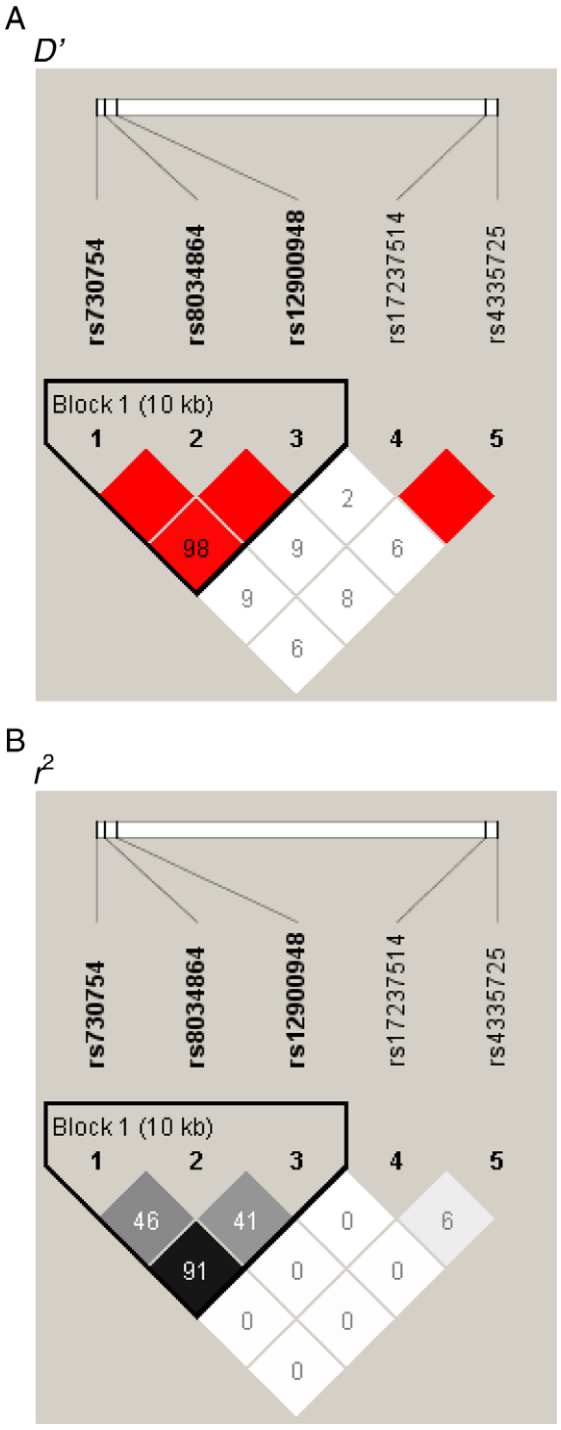

Fig. 5. Linkage disequilibrium plots for unrelated case-control cohort from Central Greece. Haplotype blocks were constructed in Haploview using the method proposed by Gabriel et al. (2002). Boxes were shaded increasingly darker to represent higher percentage of LD and the numbers listed in each square represent the D' (A) and r^2 values (B) unless the box is completely shaded in representing complete LD. A single haplotype block was generated for this cohort.

expression in mouse (Chauvet, Bois-Joyeux, & Danan, 2002; Liu et al., 2008; Zhu et al., 2006). Similarly, a limitation of using mRNA derived from lymphoblastoid cell lines is that while it may be possible to gain information that reflects systemic changes in *RORA* expression, these results may be tissue specific and therefore, may not be fully reflective of expression changes in the retina or retinal pigment epithelium (RPE) (Nica & Dermitzakis, 2008) Therefore, in order to determine whether or not *RORA* expression is truly correlated with neovascular AMD, further studies need to be conducted on a greater number of patient samples examining not only the levels of *RORA* but also the specific transcripts of *RORA* expressed in the various cell types of the retina and cells involved in the process of neovascularization (including for example, endothelial cells and immune infiltrates). In addition, evaluating the functional consequence of lack of *RORA* gene expression in a model system such as mouse may provide further insight into its role in retinal diseases such as AMD.

RORA has been shown to be ubiquitously expressed but with tissue specific isoform expression (Chauvet et al., 2002; Liu et al., 2008; Zhu et al., 2006). Immunohistochemical analysis of normal mouse retina showed *RORA* expression in the ganglion cell layer and inner nuclear layer (Fujieda, Bremner, Mears, & Sasaki, 2009; Ino, 2004; Steinmayr et al., 1998). Ganglion cell layer neurons have been shown by Medeiros and Curcio to be reduced by nearly 50% in eyes of patients with neovascular AMD compared to eyes from individuals with no AMD (Medeiros & Curcio, 2001). Further, *RORA* has been co-localized with cone specific markers and demonstrated to play an important role in the development of photoreceptors by synergistically regulating the expression of several cone genes, including *S-* and *M-opsin*, along with *CRX* in the mouse (Fujieda et al., 2009). Studies using the *RORA* deficient staggerer mouse show that *RORA* is important but not essential for cone development, as the retina of the staggerer mouse does not exhibit a difference in cone density nor a difference in other cell types compared to wild-type mice (Fujieda et al., 2009; Steinmayr et al., 1998). The role of *RORA* in the aging retina of the adult staggerer mouse has yet to be established due to lethality in early life (Fujieda et al., 2009).

In addition to the regulation of cholesterol/lipid metabolism, data suggest an inhibitory role for *RORA* in inflammation and angiogenesis, cellular processes that have also been implicated in the development and progression of neovascular AMD (Anderson, Mullins, Hageman, & Johnson, 2002; Besnard et al., 2001, 2002; Boukhtouche et al., 2004, 2006; Conley et al., 2005; Hageman et al., 2001; Johnson, 2005; Klein et al., 2003; Lau et al., 2008; Zhu et al., 2006). Macrophages isolated from the staggerer mouse were shown to have increased mRNA expression of the inflammatory cytokines interleukin-1 alpha, interleukin-1 beta, interleukin-6, and tumor necrosis factor-alpha (TNF-α) (Kopmels et al., 1990, 1991, 1992). This phenotype has been linked to *RORA*-mediated transcriptional inhibition of the pro-inflammatory transcription factor nuclear factor kappa B (NFκB) (Delerive et al., 2001). Moreover, *RORA* isoforms 1 and 4 have been shown to suppress the activation of NFκB by TNF-α and to suppress TNF-α induced expression of the cell adhesion molecules vascular cell adhesion molecule and the intracellular adhesion molecule in human endothelial cells (Migita et al., 2004). Staggerer mice also exhibited decreased angiogenesis in response to ischemia induced by femoral artery ligation (Besnard et al., 2001). It is therefore plausible that genetic variants of *RORA* might affect AMD risk through a combination of multiple pathways in addition to the regulation of cholesterol.

Given the number of processes/pathways in which *RORA* functions and the significance of association between *RORA* and neovascular AMD, it is unlikely that *RORA* alone contributes to the sequelae of events in neovascular AMD but rather that genes regulated by *RORA*, or those that regulate *RORA*, may influence the disease. Therefore, although one gene may be modestly associated with AMD risk, it may be the combination of variants within sets of genes that can lead to small changes in the way the genes/proteins interact, which, when combined with environmental effects, can have a huge impact on biological systems culminating in disease with age (Chen et al., 2008). As a result, the investigation of

Table 8
Haplotype analysis of *RORA* in the Greek cohort.

Gabriel rule Order	rs730754	rs8034864	rs12900948	UCLR odds ratio (95% C.I.)	UCLR *p*-value
Neovascular + dry vs. normal					
Block 1 – additive model					
*h*1	A	C	A	0.915 (0.803–1.043)	0.1845
*h*2	G	A	G	1.093 (0.959–1.246)	0.1845
*h*3	G	C	G	1.166 (0.934–1.456)	0.1745
Block 1 – dominant model					
*h*1	A	C	A	0.960 (0.756–1.220)	0.7396
*h*2	G	A	G	1.188 (0.978–1.443)	0.0832
*h*3	G	C	G	1.292 (0.877–1.903)	0.1958

Order	rs17237514	rs4335725	UCLR odds ratio (95% C.I.)	UCLR *p*-value
Block 4 – recessive model				
*h*1	A	G	0.963 (0.657–1.411)	0.8455
*h*2	A	A	0.826 (0.558–1.223)	0.3409
*h*3	G	G	1.266 (0.822–1.948)	0.2843

Order	rs730754	rs8034864	rs12900948	UCLR odds ratio (95% C.I.)	UCLR *p*-value
Neovascular vs. normal					
Block 1 – additive model					
*h*1	A	C	A	0.860 (0.734–1.008)	0.0622
*h*2	G	A	G	1.162 (0.992–1.361)	0.0622
*h*3	G	C	G	1.203 (0.925–1.565)	0.1670
Block 1 – dominant model					
*h*1	A	C	A	1.063 (0.800–1.413)	0.6724
*h*2	G	A	G	1.470 (1.148–1.882)	0.0022
*h*3	G	C	G	1.639 (1.032–2.603)	0.0363

Order	rs17237514	rs4335725	UCLR odds ratio (95% C.I.)	UCLR *p*-value
Block 4 – recessive model				
*h*1	A	G	0.885 (0.579–1.353)	0.5719
*h*2	A	A	0.827 (0.535–1.277)	0.3908
*h*3	G	G	1.150 (0.703–1.881)	0.5774

Order	rs730754	rs8034864	rs12900948	UCLR Odds Ratio (95% C.I.)	UCLR *p*-value
Neovascular vs. dry					
Block 1 – additive model					
*h*1	A	C	A	0.890 (0.752–1.055)	0.1788
*h*2	G	A	G	1.123 (0.948–1.330)	0.1788
*h*3	G	C	G	1.043 (0.786–1.383)	0.7721
Block 1 – dominant model					
*h*1	A	C	A	1.233 (0.922–1.649)	0.1573
*h*2	G	A	G	1.584 (1.204–2.085)	0.0010
*h*3	G	C	G	1.718 (1.017–2.905)	0.0432

Order	rs17237514	rs4335725	UCLR odds ratio (95% C.I.)	UCLR *p*-value
Block 4 – recessive model				
*h*1	A	G	0.818 (0.516–1.297)	0.3931
*h*2	A	A	0.991 (0.617–1.592)	0.9697
*h*3	G	G	0.783 (0.461–1.330)	0.3654

Abbreviation: UCLR, Unconditional Logistic Regression.

RORA related pathways and gene networks may lead to a better understanding of the pathophysiology of AMD (Figs. 1 and 6).

In this study, we observed a statistically significant interaction between *RORA* and the *ARMS2/HTRA1* locus. This finding was prospectively validated in two nested case-control cohorts (D. Schaumberg et al., paper under review). To date, the *ARMS2/HTRA1* locus is the region most significantly associated with neovascular AMD (Fisher et al., 2005; Shuler et al., 2007; Zhang et al., 2008), however, the pathway in which it functions has yet to be elucidated. This interaction suggests that *RORA* may be functioning in a similar, an overlapping, or the same pathway as *ARMS2/HTRA1* and opens up new avenues of investigation based upon the known roles of *RORA*.

Similarly, network investigation of *RORA*, in combination with *HTRA1* and the putative AMD-associated genes discovered by microarray gene expression analysis, provides further areas of study interest, some of which have been corroborated independently by different experimental means. For example, network analysis of our significant microarray genes (Fig. 1) implicated a role for transforming growth factor β (TGFβ) family members in AMD. TGFβ has been suggested to play a role in AMD by controlling secretion of vascular endothelial growth factor by RPE cells

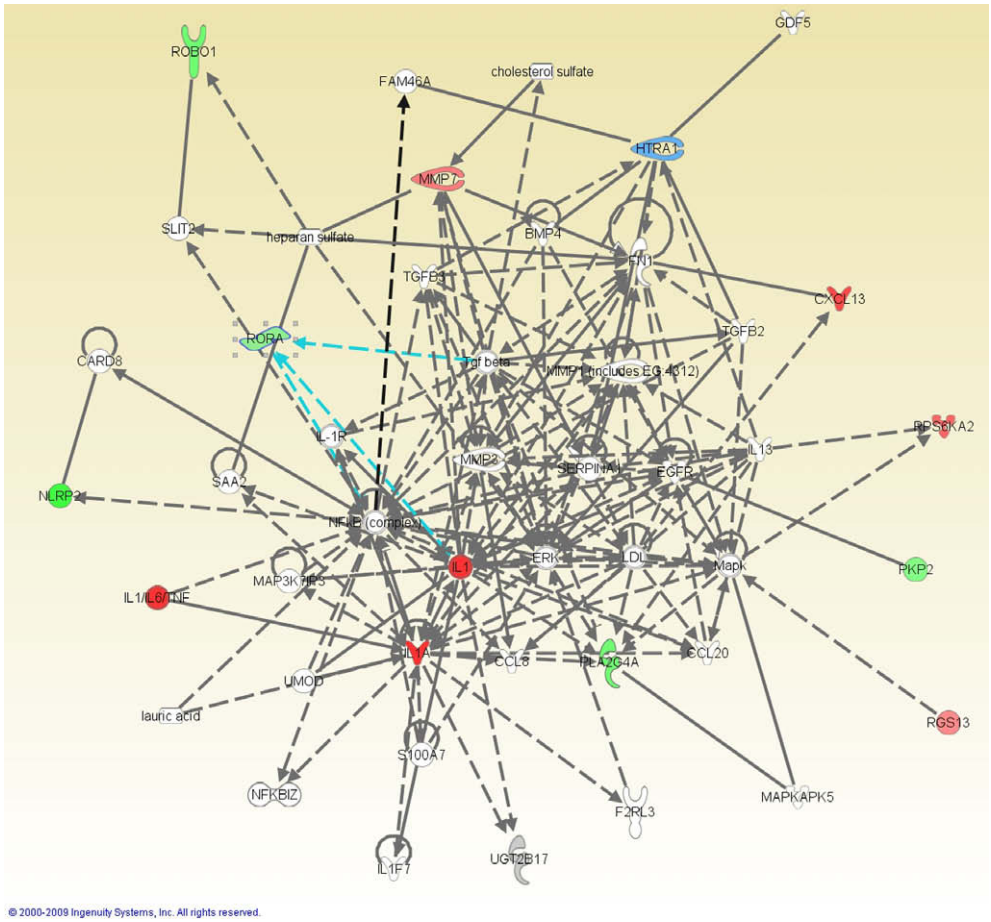

Fig. 6. IPA-generated network containing microarray genes that were identified as significant and that showed a greater than 2-fold difference when comparing neovascular AMD patients and their unaffected siblings with the addition of *HTRA1* and *HTRA1* interacting molecules. The molecules which are shaded are those that were identified in our study. Green indicates down-regulation while red indicates up-regulation when comparing affected to unaffected siblings. HTRA1 is indicated in blue. Solid lines indicate direct relationships and dotted lines indicate indirect relationships as identified in previously published literature (http://www.ingenuity.com/index.html). The individual shapes represent the family of molecule, for example, the shape of *RORA* indicates a ligand-dependent nuclear receptor. A full listing of these proteins, their official name, and the family of molecules to which they belong can be found in Supplementary Table 5. (For interpretation of the references to colour in this figure legend, the reader is referred to the web version of this article.)

(Nagineni et al., 2003). The addition of *HTRA1* to our network analysis further suggested specific members of the TGFβ family, *TGFβ2* and *TGFβ3*, that may be involved in AMD pathophysiology (Fig. 6). This example underscores the importance of examining gene–gene interaction along with network analysis data as tools in the investigation of mechanisms underlying AMD.

Another potential result of genetic variation(s) in *RORA* is the *cis* or *trans* regulation of a nearby locus, a distant gene, or the indirect regulation of a gene by means of influencing a regulatory locus (for review please see Ioannidis, Thomas, & Daly, 2009). In any of these scenarios one can hypothesize that variation within *RORA* could affect transcription of another gene(s) that in turn would influence the development and progression of AMD. Therefore, we investigated the association of the *RORA* SNPs found to be significant in our study (either directly or those within a significant haplotype) with eQTLs. Of our 5 SNPs, rs8034864, rs730754, and rs4335725 were present in the database but none were significantly associated with transcript expression (Supplementary Table 6). However, this is not surprising based on our haplotype analysis demonstrating that these SNPs are likely not individually causal.

A caveat in the investigation of *RORA* linked eQTLs is that current studies are limited by the available genome wide association and gene expression microarray platforms, thus limiting the amount of genetic variation and genes that are assayed. For example, the most significant SNP in the unrelated case-control Greek population, rs12900948, was not included in the database. As increasing data becomes available, the study of *RORA* linked eQTLs may yield interesting information regarding proteins and pathways involved in AMD.

In summary, this is the first report of a genetic association between *RORA* and neovascular AMD. The identification of *RORA* alleles and haplotypes significantly associated with neovascular AMD, coupled with linkage and gene expression data, suggests an important role for *RORA* in the aging retina. Additionally, the overlap between pathways in which *RORA* plays a role and those believed to underlie AMD pathophysiology suggests that *RORA* and the pathways in which it functions merit further investigation.

Acknowledgments

We thank all the families and subjects described in this study for their willing participation. We would like to thank the generous support from the Lincy Fund, the Marion W. and Edward F. Knight Age-Related Macular Degeneration Fund, the Massachusetts Lions, Friends of the Massachusetts Eye and Ear Infirmary, Genetics of Age-Related Macular Degeneration Fund, Eannelli for Macular Degeneration Fund, Research to Prevent Blindness, NIH Grants EY014458, EY14104, and EY017362 and Hope for Vision.

Appendix A. Supplementary material

Supplementary data associated with this article can be found, in the online version, at doi:10.1016/j.visres.2009.09.016.

References

Abecasis, G. R., Yashar, B. M., Zhao, Y., Ghiasvand, N. M., Zareparsi, S., Branham, K. E. H., et al. (2004). Age-related macular degeneration: A high-resolution genome scan for susceptibility loci in a population enriched for late-stage disease. *Human Molecular Genetics*, 482–494.

Allikmets, R. (2000). Further evidence for an association of ABCR alleles with age-related macular degeneration. The international ABCR screening consortium. *American Journal of Human Genetics, 67*, 487–491.

Allikmets, R., Bergen, A. A., Dean, M., Guymer, R. H., Hageman, G. S., Klaver, C. C., et al. (2009). Geographic atrophy in age-related macular degeneration and TLR3. *New England Journal of Medicine, 360*, 2252–2254.

Allikmets, R., Shroyer, N. F., Singh, N., Seddon, J. M., Lewis, R. A., Bernstein, P. S., et al. (1997). Mutation of the Stargardt disease gene (ABCR) in age-related macular degeneration. *Science, 277*, 1805–1807.

Anderson, D. H., Mullins, R. F., Hageman, G. S., & Johnson, L. V. (2002). A role of local inflammation in the formation of drusen in the aging eye. *American Journal of Ophthalmology*, 411–431.

Anderson, D. H., Ozaki, S., Nealon, M., Neitz, J., Mullins, R. F., Hageman, G. S., et al. (2001). Local cellular sources of apolipoprotein E in the human retina and retinal pigmented epithelium: implications for the process of drusen formation. *American Journal of Ophthalmologya, 131*, 767–781.

AREDS Research Group. (2000). *Risk factors associated with age-related macular degeneration: A case-control study in the age-related eye disease study*: AREDS Report No. 3, pp. 2224–2232.

Ayyagari, R., Zhang, K., Hutchinson, A., Yu, Z., Swaroop, A., Kakuk, L. E., et al. (2001). Evaluation of the ELOVL4 gene in patients with age-related macular degeneration. *Ophthalmic Genetics, 22*, 233–239.

Baird, P. N., Guida, E., Chu, D. T., Vu, H. T., & Guymer, R. H. (2004). The epsilon2 and epsilon4 alleles of the apolipoprotein gene are associated with age-related macular degeneration. *Investigative Ophthalmology and Visual Science, 45*, 1311–1315.

Baker, M. L., Wang, J. J., Rogers, S., Klein, R., Kuller, L. H., Larsen, E. K., et al. (2009). Early age-related macular degeneration, cognitive function, and dementia: The cardiovascular health study. *Archives of Ophthalmology, 127*, 667–673.

Besnard, S., Bakouche, J., Lemaigre-Dubreuil, Y., Mariani, J., Tedgui, A., & Henrion, D. (2002). Smooth muscle dysfunction in resistance arteries of the staggerer mouse, a mutant of the nuclear receptor RORalpha. *Circulation Research, 90*, 820–825.

Besnard, S., Silvestre, J. S., Duriez, M., Bakouche, J., Lemaigre-Dubreuil, Y., Mariani, J., et al. (2001). Increased ischemia-induced angiogenesis in the staggerer mouse, a mutant of the nuclear receptor RORalpha. *Circulation Research, 89*, 1209–1215.

Bolstad, B. M., Irizarry, R. A., Astrand, M., & Speed, T. P. (2003). A comparison of normalization methods for high density oligonucleotide array data based on variance and bias. *Bioinformatics, 19*, 185–193.

Boukhtouche, F., Mariani, J., & Tedgui, A. (2004). The "CholesteROR" protective pathway in the vascular system. *Arteriosclerosis, Thrombosis, and Vascular Biology, 24*, 637–643.

Boukhtouche, F., Vodjdani, G., Jarvis, C. I., Bakouche, J., Staels, B., Mallet, J., et al. (2006). Human retinoic acid receptor-related orphan receptor alpha1 overexpression protects neurones against oxidative stress-induced apoptosis. *Journal of Neurochemistry, 96*, 1778–1789.

Chauvet, C., Bois-Joyeux, B., Berra, E., Pouyssegur, J., & Danan, J. L. (2004). The gene encoding human retinoic acid-receptor-related orphan receptor alpha is a target for hypoxia-inducible factor 1. *Biochemical Journal – London, 384*, 79–85.

Chauvet, C., Bois-Joyeux, B., & Danan, J. L. (2002). Retinoic acid receptor-related orphan receptor (ROR) alpha4 is the predominant isoform of the nuclear receptor RORalpha in the liver and is up-regulated by hypoxia in HepG2 human hepatoma cells. *Biochemical Journal – London, 364*, 449–456.

Chauvet, C., Bois-Joyeux, B., Fontaine, C., Gervois, P., Bernard, M. A., Staels, B., et al. (2005). The gene encoding fibrinogen-beta is a target for retinoic acid receptor-related orphan receptor alpha. *Molecular Endocrinology, 19*, 2517–2526.

Chen, Y., Zhu, J., Lum, P. Y., Yang, X., Pinto, S., MacNeil, D. J., et al. (2008). Variations in DNA elucidate molecular networks that cause disease. *Nature, 452*, 429–435.

Cho, Y., Wang, J. J., Chew, E. Y., Ferris, F.L., Mitchell, P., Chan, C.C., & Tuo, J. (2009). Toll-like receptor polymorphisms and age-related macular degeneration: Replication in three case-control samples. *Investigative Ophthalmology and Visual Science*.

Conley, Y. P., Thalamuthu, A., Jakobsdottir, J., Weeks, D. E., Mah, T., Ferrell, R. E., et al. (2005). Candidate gene analysis suggests a role for fatty acid biosynthesis and regulation of the complement system in the etiology of age-related maculopathy. *Human Molecular Genetics*, 1991–2002.

Cookson, W., Liang, L., Abecasis, G., Moffatt, M., & Lathrop, M. (2009). Mapping complex disease traits with global gene expression. *Nature Reviews Genetics, 10*, 184–194.

De La Paz, M. A., Guy, V. K., Abou-Donia, S., Heinis, R., Bracken, B., Vance, J. M., et al. (1999). Analysis of the Stargardt disease gene (ABCR) in age-related macular degeneration. *Ophthalmology, 106*, 1531–1536.

DeAngelis, M. M., Ji, F., Adams, S., Morrison, M. A., Harring, A. J., Sweeney, M. O., et al. (2008). Alleles in the HtrA serine peptidase 1 gene alter the risk of neovascular age-related macular degeneration. *Ophthalmology, 115*, 1209–1215.

DeAngelis, M. M., Ji, F., Kim, I. K., Adams, S., Capone, A., Jr., Ott, J., et al. (2007). Cigarette smoking, CFH, APOE, ELOVL4, and risk of neovascular age-related macular degeneration. *Archives of Ophthalmology, 125*, 49–54.

Delerive, P., Monte, D., Dubois, G., Trottein, F., Fruchart-Najib, J., Mariani, J., et al. (2001). The orphan nuclear receptor RORalpha is a negative regulator of the inflammatory response. *EMBO Reports, 2*, 42–48.

Despriet, D. D., Bergen, A. A., Merriam, J. E., Zernant, J., Barile, G. R., Smith, R. T., et al. (2008). Comprehensive analysis of the candidate genes CCL2, CCR2, and TLR4 in age-related macular degeneration. *Investigative Ophthalmology and Visual Science, 49*, 364–371.

Dewan, A., Liu, M., Hartman, S., Zhang, S. S., Liu, D. T., Zhao, C., et al. (2006). HTRA1 promoter polymorphism in wet age-related macular degeneration. *Science, 314*, 989–992.

Ding, X., Patel, M., & Chan, C. C. (2009). Molecular pathology of age-related macular degeneration. *Progress in Retinal and Eye Research, 28*, 1–18.

Dixon, A. L., Liang, L., Moffatt, M. F., Chen, W., Heath, S., Wong, K. C., et al. (2007). A genome-wide association study of global gene expression. *Nature Genetics, 39*, 1202–1207.

Edwards, A. O., Chen, D., Fridley, B. L., James, K. M., Wu, Y., Abecasis, G., et al. (2008). Toll-like receptor polymorphisms and age-related macular degeneration. *Investigative Ophthalmology and Visual Science, 49*, 1652–1659.

Edwards, A. O., Ritter, R., III, Abel, K. J., Manning, A., Panhuysen, C., & Farrer, L. A. (2005). Complement factor H polymorphism and age-related macular degeneration. *Science, 308*, 421–424.

Edwards, A. O., Swaroop, A., & Seddon, J. M. (2009). Geographic atrophy in age-related macular degeneration and TLR3. *New England Journal of Medicine, 360*, 2254–2255.

Fisher, S. A., Abecasis, G. R., Yashar, B. M., Zareparsi, S., Swaroop, A., Iyengar, S. K., et al. (2005). Meta-analysis of genome scans of age-related macular degeneration. *Human Molecular Genetics, 14*, 2257–2264.

Fujieda, H., Bremner, R., Mears, A. J., & Sasaki, H. (2009). Retinoic acid receptor-related orphan receptor alpha regulates a subset of cone genes during mouse retinal development. *Journal of Neurochemistry, 108*, 91–101.

Gabriel, S. B., Schaffner, S. F., Nguyen, H., Moore, J. M., Roy, J., Blumenstiel, B., et al. (2002). The structure of haplotype blocks in the human genome. *Science, 296*, 2225–2229.

Guymer, R. H., Heon, E., Lotery, A. J., Munier, F. L., Schorderet, D. F., Baird, P. N., et al. (2001). Variation of codons 1961 and 2177 of the Stargardt disease gene is not associated with age-related macular degeneration. *Archives of Ophthalmology, 119*, 745–751.

Haddad, S., Chen, C. A., Santangelo, S. L., & Seddon, J. M. (2006). The genetics of age-related macular degeneration: A review of progress to date. *Survey of Ophthalmology, 51*, 316–363.

Hageman, G. S., Anderson, D. H., Johnson, L. V., Hancox, L. S., Taiber, A. J., Hardisty, L. I., et al. (2005). A common haplotype in the complement regulatory gene factor H (HF1/CFH) predisposes individuals to age-related macular degeneration. *Proceedings of the National Academy of Sciences USA, 102*, 7227–7232.

Hageman, G. S., Luthert, P. J., Victor Chong, N. H., Johnson, L. V., Anderson, D. H., & Mullins, R. F. (2001). An integrated hypothesis that considers drusen as biomarkers of immune-mediated processes at the RPE-Bruch's membrane interface in aging and age-related macular degeneration. *Progress in Retinal and Eye Research, 20*, 705–732.

Haines, J. L., Hauser, M. A., Schmidt, S., Scott, W. K., Olson, L. M., Gallins, P., et al. (2005). Complement factor H variant increases the risk of age-related macular degeneration. *Science, 308*, 419–421.

Hastings, P. J., Lupski, J. R., Rosenberg, S. M., & Ira, G. (2009). Mechanisms of change in gene copy number. *Nature Reviews Genetics, 10*, 551–564.

Hollams, E. M., Giles, K. M., Thomson, A. M., & Leedman, P. J. (2002). mRNA stability and the control of gene expression: Implications for human disease. *Neurochemical Research, 27*, 957–980.

Hubbard, T. J., Aken, B. L., Ayling, S., Ballester, B., Beal, K., Bragin, E., et al. (2009). Ensembl 2009. *Nucleic Acids Research, 37*, D690–D697.

Ino, H. (2004). Immunohistochemical characterization of the orphan nuclear receptor RORalpha in the mouse nervous system. *Journal of Histochemistry and Cytochemistry, 52*, 311–323.

Ioannidis, J. P., Thomas, G., & Daly, M. J. (2009). Validating, augmenting and refining genome-wide association signals. *Nature Reviews Genetics, 10*, 318–329.

Irizarry, R. A., Hobbs, B., Collin, F., Beazer-Barclay, Y. D., Antonellis, K. J., Scherf, U., et al. (2003). Exploration, normalization, and summaries of high density oligonucleotide array probe level data. *Biostatistics, 4*, 249–264.

Iyengar, S. K., Song, D., Klein, B. E., Klein, R., Schick, J. H., Humphrey, J., et al. (2004). Dissection of genomewide-scan data in extended families reveals a major locus and oligogenic susceptibility for age-related macular degeneration. *American Journal of Human Genetics, 74*, 20–39.

Jakobsdottir, J., Conley, Y. P., Weeks, D. E., Mah, T. S., Ferrell, R. E., & Gorin, M. B. (2005). Susceptibility genes for age-related maculopathy on chromosome 10q26. *American Journal of Human Genetics, 77*, 389–407.

Jakobsdottir, J., Gorin, M. B., Conley, Y. P., Ferrell, R. E., & Weeks, D. E. (2009). Interpretation of genetic association studies: Markers with replicated highly significant odds ratios may be poor classifiers. *PLoS Genetics, 5*, e1000337.

Javitt, N. B., & Javitt, J. C. (2009). The retinal oxysterol pathway: A unifying hypothesis for the cause of age-related macular degeneration. *Current Opinion in Ophthalmology, 20*, 151–157.

Jetten, A. M., & Ueda, E. (2002). Retinoid-related orphan receptors (RORs): Roles in cell survival, differentiation and disease. *Cell Death and Differentiation, 9*, 1167–1171.

Johnson, E. J. (2005). Obesity, Lutein metabolism, and age-related macular degeneration: A web of connections. *Nutrition Reviews*, 9–15.

Jun, G., Klein, B. E., Klein, R., Fox, K., Millard, C., Capriotti, J., et al. (2005). Genome-wide analyses demonstrate novel loci that predispose to drusen formation. *Investigative Ophthalmology and Visual Science, 46*, 3081–3088.

Kallen, J. A., Schlaeppi, J. M., Bitsch, F., Geisse, S., Geiser, M., Delhon, I., et al. (2002). X-ray structure of the hRORalpha LBD at 1.63 A: Structural and functional data that cholesterol or a cholesterol derivative is the natural ligand of RORalpha. *Structure, 10*, 1697–1707.

Kanda, A., Chen, W., Othman, M., Branham, K. E., Brooks, M., Khanna, R., et al. (2007). A variant of mitochondrial protein LOC387715/ARMS2, not HTRA1, is strongly associated with age-related macular degeneration. *Proceedings of the National Academy of Sciences USA, 104*, 16227–16232.

Kenealy, S. J., Schmidt, S., Agarwal, A., Postel, E. A., De La Paz, M. A., Pericak-Vance, M. A., et al. (2004). Linkage analysis for age-related macular degeneration supports a gene on chromosome 10q26. *Molecular Vision, 10*, 57–61.

Klaver, C. C., Kliffen, M., Van Duijn, C. M., Hofman, A., Cruts, M., Grobbee, D. E., et al. (1998). Genetic association of apolipoprotein E with age-related macular degeneration. *American Journal of Human Genetics, 63*, 200–206.

Klein, R., Klein, B. E. K., Tomany, S. C., Danforth, L. G., & Cruickshanks, K. J. (2003). Relation of statin use to the 5-year incidence and progression of age-related maculopathy. *Archives of Ophthalmology*, 1151–1155.

Klein, R., Klein, B. E. K., & Jensen, S. C. (1997). The relation of cardiovascular disease and its risk factor to the 5-year incidence of age-related maculopathy. *Ophthalmology, 104*, 1804–1812.

Klein, R., Klein, B. E. K., Tomany, S. C., & Moss, S. E. (2002). Ten-year incidence of age-related maculopathy and smoking and drinking. The beaver dam eye study. *American Journal of Epidemiology, 156*, 589–598.

Klein, R. J., Zeiss, C., Chew, E. Y., Tsai, J. Y., Sackler, R. S., Haynes, C., et al. (2005). Complement factor H polymorphism in age-related macular degeneration. *Science, 308*, 385–389.

Kopmels, B., Mariani, J., Delhaye-Bouchaud, N., Audibert, F., Fradelizi, D., & Wollman, E. E. (1992). Evidence for a hyperexcitability state of staggerer mutant mice macrophages. *Journal of Neurochemistry, 58*, 192–199.

Kopmels, B., Mariani, J., Taupin, V., Delhaye-Bouchaud, N., & Wollman, E. E. (1991). Differential IL-6 mRNA expression by stimulated peripheral macrophages of Staggerer and Lurcher cerebellar mutant mice. *European Cytokine Network, 2*, 345–353.

Kopmels, B., Wollman, E. E., Guastavino, J. M., Delhaye-Bouchaud, N., Fradelizi, D., & Mariani, J. (1990). Interleukin-1 hyperproduction by in vitro activated peripheral macrophages from cerebellar mutant mice. *Journal of Neurochemistry, 55*, 1980–1985.

Lau, P., Fitzsimmons, R. L., Raichur, S., Wang, S. C., Lechtken, A., & Muscat, G. E. (2008). The orphan nuclear receptor, RORalpha, regulates gene expression that controls lipid metabolism: Staggerer (SG/SG) mice are resistant to diet-induced obesity. *Journal of Biological Chemistry, 283*, 18411–18421.

Lewin, A. S. (2009). Geographic atrophy in age-related macular degeneration and TLR3. *New England Journal of Medicine, 360*, 2251–2256.

Li, M., tmaca-Sonmez, P., Othman, M., Branham, K. E., Khanna, R., Wade, M. S., et al. (2006). CFH haplotypes without the Y402H coding variant show strong association with susceptibility to age-related macular degeneration. *Nature Genetics, 38*, 1049–1054.

Liew, G., Mitchell, P., & Wong, T. Y. (2009). Geographic atrophy in age-related macular degeneration and TLR3. *New England Journal of Medicine, 360*, 2252–2256.

Liu, A. C., Tran, H. G., Zhang, E. E., Priest, A. A., Welsh, D. K., & Kay, S. A. (2008). Redundant function of REV-ERBalpha and beta and non-essential role for Bmal1 cycling in transcriptional regulation of intracellular circadian rhythms. *PLoS Genetics, 4*, e1000023.

Lonnstedt, I., & Speed, T. P. (2002). Replicated microarray data. *Statistica Sinica, 12*, 31–46.

Lupski, J. R. (2007). Genomic rearrangements and sporadic disease. *Nature Genetics, 39*, S43–S47.

Maddox, D. M., Vessey, K. A., Yarbrough, G. L., Invergo, B. M., Cantrell, D. R., Inayat, S., et al. (2008). Allelic variance between GRM6 mutants, Grm6nob3 and Grm6nob4 results in differences in retinal ganglion cell visual responses. *Journal of Physiology, 586*, 4409–4424.

Majewski, J., Schultz, D. W., Weleber, R. G., Schain, M. B., Edwards, A. O., Matise, T. C., et al. (2003). Age-related macular degeneration – A genome scan in extended families. *American Journal of Human Genetics*, 540–550.

Mamontova, A., Seguret-Mace, S., Esposito, B., Chaniale, C., Bouly, M., Delhaye-Bouchaud, N., et al. (1998). Severe atherosclerosis and hypoalpha-lipoproteinemia in the staggerer mouse, a mutant of the nuclear receptor RORalpha. *Circulation, 98*, 2738–2743.

Margulies, E. H., & Birney, E. (2008). Approaches to comparative sequence analysis: Towards a functional view of vertebrate genomes. *Nature Reviews Genetics, 9*, 303–313.

McGwin, G., Xie, A., & Owsley, C. (2005). The use of cholesterol-lowering medications and age-related macular degeneration. *Ophthalmology*, 488–494.

Medeiros, N. E., & Curcio, C. A. (2001). Preservation of ganglion cell layer neurons in age-related macular degeneration. *Investigative Ophthalmology and Visual Science, 42*, 795–803.

Migita, H., Satozawa, N., Lin, J. H., Morser, J., & Kawai, K. (2004). RORalpha1 and RORalpha4 suppress TNF-alpha-induced VCAM-1 and ICAM-1 expression in human endothelial cells. *FEBS Letters, 557*, 269–274.

Moffatt, M. F., Kabesch, M., Liang, L., Dixon, A. L., Strachan, D., Heath, S., et al. (2007). Genetic variants regulating ORMDL3 expression contribute to the risk of childhood asthma. *Nature, 448*, 470–473.

Mullins, R. F., Russell, S. R., Anderson, D. H., & Hageman, G. S. (2000). Drusen associated with aging and age-related macular degeneration contain proteins common to extracellular deposits associated with atherosclerosis, elastosis, amyloidosis, and dense deposit disease. *FASEB Journal, 14*, 835–846.

Nagineni, C. N., Samuel, W., Nagineni, S., Pardhasaradhi, K., Wiggert, B., Detrick, B., et al. (2003). Transforming growth factor-beta induces expression of vascular endothelial growth factor in human retinal pigment epithelial cells: Involvement of mitogen-activated protein kinases. *Journal of Cellular Physiology, 197*, 453–462.

Nica, A. C., & Dermitzakis, E. T. (2008). Using gene expression to investigate the genetic basis of complex disorders. *Human Molecular Genetics, 17*, R129–R134.

Risch, N., & Zhang, H. (1995). Extreme discordant sib pairs for mapping quantitative trait loci in humans. *Science, 268*, 1584–1589.

Risch, N. J., & Zhang, H. (1996). Mapping quantitative trait loci with extreme discordant sib pairs: Sampling considerations. *American Journal of Human Genetics, 58*, 836–843.

Rivera, A., Fisher, S. A., Fritsche, L. G., Keilhauer, C. N., Lichtner, P., Meitinger, T., et al. (2005). Hypothetical LOC387715 is a second major susceptibility gene for age-related macular degeneration, contributing independently of complement factor H to disease risk. *Human Molecular Genetics, 14*, 3227–3236.

Sallo, F. B., Bereczki, E., Csont, T., Luthert, P. J., Munro, P., Ferdinandy., et al. (2009). Bruch's membrane changes in transgenic mice overexpressing the human biglycan and apolipoprotein b-100 genes. *Experimental Eye Research.*

Schick, J. H., Iyengar, S. K., Klein, B. E., Klein, R., Reading, K., Liptak, R., et al. (2003). A whole-genome screen of a quantitative trait of age-related maculopathy in sibships from the beaver dam eye study. *American Journal of Human Genetics, 72*, 1412–1424.

Schmidt, S., Klaver, C. C., Saunders, A. M., Postel, E. A., De La Paz, M. A., Agarwal, N., et al. (2002). A pooled case-control study of the apolipoprotein E (APOE) gene in age-related maculopathy. *Ophthalmic Genetics*, 209–223.

Schmidt, S., Scott, W. K., Postel, E. A., Agarwal, A., Hauser, E. R., De La Paz, M. A., et al. (2004). Ordered subset linkage analysis supports a susceptibility locus for age-related macular degeneration on chromosome 16p12. *BMC Genetics, 5*, 18.

Schultz, D. W., Klein, M. L., Humpert, A., Majewski, J., Schain, M., Weleber, R. G., et al. (2003). Lack of an association of apolipoprotein E gene polymorphisms with familial age-related macular degeneration. *Archives of Ophthalmology, 121*, 679–683.

Seddon, J. M., Santangelo, S. L., Book, K., Chong, S., & Cote, J. (2003). A genome wide scan for age-related macular degeneration provides evidence for linkage to several chromosomal regions. *American Journal of Human Genetics, 73*, 780–790.

Shimada, M. K., Matsumoto, R., Hayakawa, Y., Sanbonmatsu, R., Gough, C., Yamaguchi-Kabata, Y., et al. (2009). VarySysDB: A human genetic polymorphism database based on all H-InvDB transcripts. *Nucleic Acids Research, 37*, D810–D815.

Shuler, R. K., Jr., Hauser, M. A., Caldwell, J., Gallins, P., Schmidt, S., Scott, W. K., et al. (2007). Neovascular age-related macular degeneration and its association with LOC387715 and complement factor H polymorphism. *Archives of Ophthalmology, 125*, 63–67.

Souied, E. H., Benlian, P., Amouyel, P., Feingold, J., Lagarde, J. P., Munnich, A., et al. (1998). The epsilon4 allele of the apolipoprotein E gene as a potential protective factor for exudative age-related macular degeneration. *American Journal of Ophthalmology, 125*, 353–359.

Souied, E. H., Ducroq, D., Rozet, J. M., Gerber, S., Perrault, I., Munnich, A., et al. (2000). ABCR gene analysis in familial exudative age-related macular degeneration. *Investigative Ophthalmology and Visual Science, 41*, 244–247.

Steinmayr, M., Andre, E., Conquet, F., Rondi-Reig, L., Delhaye-Bouchaud, N., Auclair, N., et al. (1998). Staggerer phenotype in retinoid-related orphan receptor alpha-deficient mice. *Proceedings of the National Academy of Sciences USA, 95*, 3960–3965.

Stone, E. M., Webster, A. R., Vandenburgh, K., Streb, L. M., Hockey, R. R., Lotery, A. J., et al. (1998). Allelic variation in ABCR associated with Stargardt disease but not age-related macular degeneration [letter]. *Nature Genetics, 20*, 328–329.

Tan, J. S., Wang, J. J., Flood, V., & Mitchell, P. (2009). Dietary fatty acids and the 10-year incidence of age-related macular degeneration: The Blue Mountains eye study. *Archives of Ophthalmology, 127*, 656–665.

Tusher, V. G., Tibshirani, R., & Chu, G. (2001). Significance analysis of microarrays applied to the ionizing radiation response. *Proceedings of the National Academy of Sciences USA, 98*, 5116–5121.

van Leeuwen, R., Vingerling, J. R., Hofman, A., de Jong, P. T., & Stricker, B. H. (2003). Cholesterol lowering drugs and risk of age related maculopathy: Prospective cohort study with cumulative exposure measurement. *BMJ, 326*, 255–256.

Voyiaziakis, E., Goldberg, I. J., Plump, A. S., Rubin, E. M., Breslow, J. L., & Huang, L. S. (1998). ApoA-I deficiency causes both hypertriglyceridemia and increased atherosclerosis in human apoB transgenic mice. *Journal of Lipid Research, 39*, 313–321.

Ware, J. H. (2006). The limitations of risk factors as prognostic tools. *New England Journal of Medicine, 355*, 2615–2617.

Wilson, H. L., Schwartz, D. M., Bhatt, H. R. F., McCulloch, C. E., & Duncan, J. L. (2004). Statin and aspirin therapy are associated with decreased rates of choroidal

neovascularization among patients with age-related macular degeneration. *American Journal of Ophthalmology*, 615–624.

Wu, Z., & Irizarry, R. A. (2004). Stochastic models inspired by hybridization theory for short oligonucleotide arrays. *Journal of Computational Biology, 12*, 882–893.

Yamada, Y., Tian, J., Yang, Y., Cutler, R. G., Wu, T., Telljohann, R. S., et al. (2008). Oxidized low density lipoproteins induce a pathologic response by retinal pigmented epithelial cells. *Journal of Neurochemistry, 105*, 1187–1197.

Yang, Z., Camp, N. J., Sun, H., Tong, Z., Gibbs, D., Cameron, D. J., et al. (2006). A variant of the HTRA1 gene increases susceptibility to age-related macular degeneration. *Science, 314*, 992–993.

Yang, Z., Stratton, C., Francis, P. J., Kleinman, M. E., Tan, P. L., Gibbs, D., et al. (2008). Toll-like receptor 3 and geographic atrophy in age-related macular degeneration. *New England Journal of Medicine, 359*, 1456–1463.

Yu, A. L., Lorenz, R. L., Haritoglou, C., Kampik, A., & Welge-Lussen, U. (2009). Biological effects of native and oxidized low-density lipoproteins in cultured human retinal pigment epithelial cells. *Experimental Eye Research, 88*, 495–503.

Zareparsi, S., Buraczynska, M., Branham, K. E. H., Shah, S., Eng, D., Li, M., Pawar, H., et al. (2005). Toll-like receptor 4 variant D299G is associated with susceptibility to age-related macular degeneration. *Human Molecular Genetics*, 1449–1455.

Zareparsi, S., Reddick, A. C., Branham, K. E., Moore, K. B., Jessup, L., Thoms, S., et al. (2004). Association of apolipoprotein E alleles with susceptibility to age-related macular degeneration in a large cohort from a single center. *Investigative Ophthalmology and Visual Science, 45*, 1306–1310.

Zhang, H., Morrison, M. A., Dewan, A., Adams, S., Andreoli, M., Huynh, N., et al. (2008). The NEI/NCBI dbGAP database: Genotypes and haplotypes that may specifically predispose to risk of neovascular age-related macular degeneration. *BMC Medical Genetics, 9*, 51.

Zhu, Y., McAvoy, S., Kuhn, R., & Smith, D. I. (2006). RORA, a large common fragile site gene, is involved in cellular stress response. *Oncogene, 25*, 2901–2908.